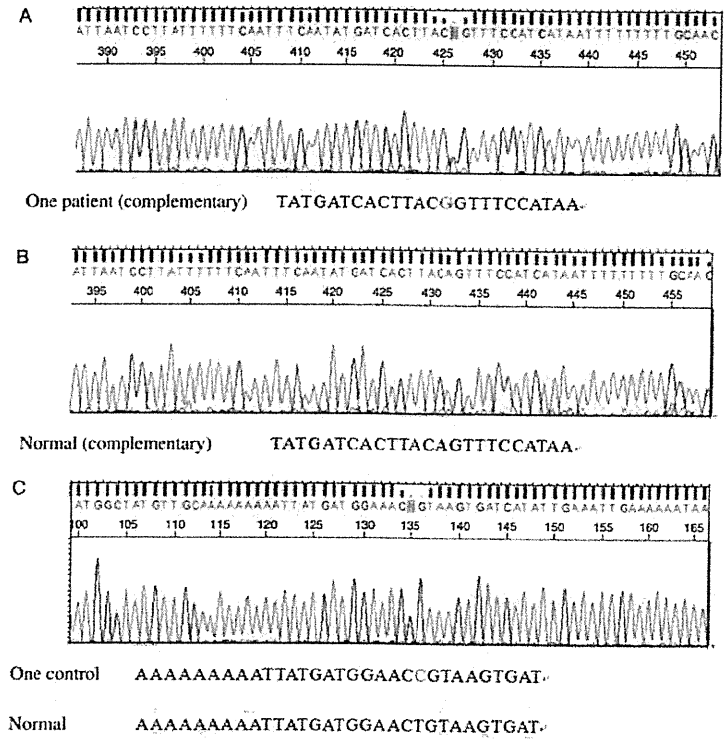

Figure 1 Nucleotide sequence results for the *SYCP3* gene in women with recurrent miscarriage and a control. (**A**) Heterozygous 657T>C mutation in exon 8 of the *SYCP3* gene of one patient with a history of six recurrent miscarriages. (**B**) Normal genotype in one patient with recurrent miscarriage. (**C**) Heterozygous 657T>C mutation in exon 8 of the *SYCP3* gene in one control with a history of one live birth and no miscarriages. From (A–C) sequences are all of the same region, and (A) and (B) sequences are complementary.

production of proteins that were mutated at the C-terminus. However, the effects of the *SYCP3* mutations on non-disjunction or the function of the synaptonemal complex have not been clear in mammals so far.

Our patient with 657T>C had repeated miscarriages with euploidy. It may be that the 657T>C mutation is a polymorphism without the specific function ascertained in the Bolor *et al.* (2009) study in humans. Further studies with larger numbers and a wide range of cases are needed to define whether the *SYCP3* mutations can be a cause of recurrent miscarriage.

Sycp3-deficient mice show complete meiotic arrest leading to male infertility (Yuan *et al.*, 2000). Miyamoto *et al.* (2003) identified in two azoospermia patients a 1 bp deletion of the *SYCP3* gene (643delA) that results in a premature stop codon and truncation of the C-terminal, coiled-coil-forming region of the SYCP3 protein. The mutant protein showed greatly reduced interaction with the wild-type protein *in vitro* (Miyamoto *et al.*, 2003). Reynolds *et al.* (2007) suggested that azoospermia associated with a decrease in the *DAZ* gene function in humans might, in part, be the consequence of failure at synapsis caused by reduced levels of the SYCP protein. However, no female patient with the 643delA mutation of SYCP3 has been reported. The infertile women might have the mutation because embryos with trisomy or monosomy except 45,X are frequently seen by PGD.

Our data showed that among the normal fetal karyotypes, XX and XY were found at a similar frequency, indicating that fetal rather than maternal karyotypes were obtained. In this study, about 90% of patients with abnormal and normal embryonic (fetal) karyotype tended to have repeat miscarriages with abnormal and normal karyotypes, respectively. The results suggest that unexplained recurrent miscarriage should be grouped as two types: one is miscarriage caused by abnormal embryonic karyotype and the other is 'real' unexplained recurrent miscarriage.

Moreover, the prognosis of a successful pregnancy for patients with an abnormal embryonic karyotype was better than for patients with a normal embryonic karyotype (Ogasawara *et al.*, 2000). No therapeutic approach to improve the rate of live birth could be found at this time (Kaandorp *et al.*, 2010). Thus, the gene associated with unexplained recurrent miscarriage with normal embryonic karyotype is more important (Suzumori and Sugiura-Ogasawara, 2010).

The results of our study suggest no clinical significance of routine screening for the presence of the *SYCP3* mutation in women with recurrent miscarriage because we detected only one benign mutation in 101 such patients. Future studies in mammalian animal models are likely to accelerate our understanding of the molecular mechanisms involved in recurrent miscarriage and will provide additional candidate genes to be screened in recurrent miscarriage patients and embryos with genetic factors.

Authors' roles

N.S., Y.O., M.N. and M.S.-O. were involved in conception and design; E.M., K.O. and C.Y-N. conducted data analysis; E.M., N.S. and M.S.-O. were involved in drafting the article. All authors agreed final approval of the version to be published.

Acknowledgements

We thank Shintaro Obayashi, M.D., Kenji Asamoto, M.D. and Kinue Katano, M.D. for organizing the collection of samples.

Funding

This study was supported by a Grant-in-Aid for Scientific Research from the Ministry of Health, Labour and Welfare (to M.S.-O.), by the Ministry of Education, Culture, Sports, Science, and Technology of Japan (to N.S.) and by the Japan Medical Association (to M.S.-O.).

References

Aarabi M, Modarressi MH, Soltanghoraee H, Behjati R, Amirjannati N, Akhondi MM. Testicular expression of synaptonemal complex protein 3 (SYCP3) messenger ribonucleic acid in 110 patients with nonobstructive azoospermia. *Fertil Steril* 2006;**86**:325–331.

Balasch J, Font J, López-Soto A, Cervera R, Jové I, Casals FJ, Vanrell JA. Antiphospholipid antibodies in unselected patients with repeated abortion. *Hum Reprod* 1990;**5**:43–46.

Bolor H, Mori T, Nishiyama S, Ito Y, Hosoba E, Inagaki H, Kogo H, Ohye T, Tsutsumi M, Kato T *et al.* Mutations of the SYCP3 gene in women with recurrent pregnancy loss. *Am J Hum Genet* 2009;**84**:14–20.

Carp H, Toder V, Aviram A, Daniely M, Mashiach S, Barkai G. Karyotype of the abortus in recurrent miscarriage. *Fertil Steril* 2001;**75**:678–682.

Coulam CB, Jeyendran RS, Fishel LA, Roussev R. Multiple thrombophilic gene mutations rather than specific gene mutations are risk factors for recurrent miscarriage. *Am J Reprod Immunol* 2006;**55**:360–368.

Farquharson RG, Pearson JF, John L. Lupus anticoagulant and pregnancy management. *Lancet* 1984;**28**:228–229.

Goodman CS, Coulam CB, Jeyendran RS, Acosta VA, Roussev R. Which thrombophilic gene mutations are risk factors for recurrent pregnancy loss? *Am J Reprod Immunol* 2006;**56**:230–236.

Harper J, Coonen E, De Rycke M, Fiorentino F, Geraedts J, Goossens V, Harton G, Moutou C, Pehlivan Budak T, Renwick P *et al.* What next for preimplantation genetic screening (PGS)? A position statement from the ESHRE PGD Consortium Steering Committee. *Hum Reprod* 2010; **25**:821–823.

Kaandorp SP, Goddijin M, van der Post JA, Hutten BA, Verhoeve HR, Hamulyák K, Mol BW, Folkeringa N, Nahuis M, Papatsonis DN *et al.* Aspirin plus heparin or aspirin alone in women with recurrent miscarriage. *N Engl J Med* 2010;**362**:1586–4166.

Miyamoto T, Hasuike S, Yogev L, Maduro MR, Ishikawa M, Westphal H, Lamb DJ. Azoospermia in patients heterozygous for a mutation in SYCP3. *Lancet* 2003;**362**:1714–1719.

Nelen W, Steegers E, Eskes T, Blom H. Genetic risk factors for unexplained recurrent pregnancy loss. *Lancet* 1996;**350**:861.

Ogasawara M, Aoki K, Matsuura E, Sasa H, Yagami Y. Antiβglycoprotein I antibodies and lupus anticoagulant in patients with recurrent pregnancy loss: prevalence and clinical association. *Lupus* 1996; **5**:587–592.

Ogasawara M, Aoki K, Okada S, Suzumori K. Embryonic karyotype of abortuses in relation to the number of previous miscarriages. *Fertil Steril* 2000;**73**:300–304.

Platteau P, Staessen C, Michiels A, Van Steirteghem A, Liebaers I, Devroey P. Preimplantation genetic diagnosis for aneuploidy screening in patients with unexplained recurrent miscarriages. *Fertil Steril* 2005; **83**:393–397.

Rai R, Regan L. Recurrent miscarriage. *Lancet* 2006;**368**:601–611.

Rey E, Kahn SR, David M, Shrier I. Thrombophilic disorders and fetal loss: a meta-analysis. *Lancet* 2003;**361**:901–908.

Reynolds N, Collier B, Bingham V, Gray NK, Cooke HJ. Translation of the synaptonemal complex component Sycp3 is enhanced *in vivo* by the germ cell specific regulator DAZI. *RNA* 2007;**13**:974–981.

Sugiura-Ogasawara M, Ozaki Y, Sato T, Suzumori N, Suzumori K. Poor prognosis of recurrent aborters with either maternal or paternal reciprocal translocation. *Fertil Steril* 2004;**81**:367–373.

Sugiura-Ogasawara M, Ozaki Y, Kitaori T, Kumagai K, Suzuki S. Midline uterine defect size correlated with miscarriage of euploid embryos in recurrent cases. *Fertil Steril* 2010;**93**:1983–1988.

Suzumori N, Sugiura-Ogasawara M. Genetic factors as a cause of miscarriage. *Curr Med Chem* 2010;**17**:3431–3437.

The American College of Obstetrics and Gynecologists. Preimplantation genetic screening for aneuploidy. *Obstet Gynecol* 2009;**113**:766–767.

Yuan L, Liu JG, Zhao J, Brundell E, Daneholt B, Hoog C. The murine SCP3 gene is required for synaptonemal complex assembly, chromosome synapsis, and male fertility. *Mol Cell* 2000;**5**:73–83.

Yuan L, Liu JG, Hoja MR, Wilbertz J, Nordqvist K, Hoog C. Female germ cell aneuploidy and embryo death in mice lacking the meiosis-specific protein SCP3. *Science* 2002;**296**:1115–1118.

J Pharmacol Sci 115, 263 – 269 (2011)

Journal of Pharmacological Sciences

Forum Minireview

Novel Findings for the Development of Drug Therapy for Various Liver Diseases:
Genetic Variation in *IL-28B* Is Associated With Response to the Therapy for Chronic Hepatitis C

Masaya Sugiyama[1,3,4], Yasuhito Tanaka[2,*], Makoto Nakanishi[1], and Masashi Mizokami[3]

[1]*Department of Biochemistry and Cell Biology,* [2]*Department of Virology & Liver Unit, Nagoya City University Graduate School of Medical Sciences, 1 Kawasumi, Mizuho, Mizuho-ku, Nagoya 467-0001, Japan*
[3]*The Research Center for Hepatitis and Immunology, National Center for Global Health and Medicine, 1-7-1 Kohnodai, Ichikawa 272-8516, Japan*
[4]*JSPS Research Fellow*

Received August 20, 2010; Accepted October 25, 2010

Abstract. Hepatitis C infection is a global health problem. Spontaneous viral clearance was observed in approximately 30% of individuals with acute infection. In the therapy using a combination of pegylated interferon-α and ribavirin, approximately 50% of chronic hepatitis C patients infected with high viremia of hepatitis C virus infection (HCV) genotype 1 reached a sustained viral response. These findings were strongly expected to reflect variations of the host genome. To reveal genetic effects against viral clearance or treatment response, four independent groups applied a genome-wide association study (GWAS) to HCV infection. These groups almost simultaneously reported a strong association of interleukin (IL)-28B polymorphisms with viral clearance or final decision of HCV therapy. The discovered single nucleotide polymorphisms (SNPs) also revealed the enigma that the viral clearance rate was dependent on ethnic type. The significant SNPs are useful for prediction prior to treatment because of the strong association with clinical outcome. In addition, the unexpected results revealed by GWAS could promote the development of a novel drug related to IL-28B. Herein, we present current understanding in regard to the relationship between host variations and clinical outcome of hepatitis C.

Keywords: hepatitis C virus, genome-wide association study, interleukin-28, interferon-λ, single nucleotide polymorphism, liver disease

1. Introduction

Chronic infection with hepatitis C virus (HCV) presents a significant health problem worldwide with approximately 3% of the world population, that is, more than 170 million people. Only 20% – 30% of HCV-infected individuals recover spontaneously. The remaining 70% – 80% going on to develop chronic infection have a significant risk for progressive liver fibrosis and subsequent liver cirrhosis (LC) and hepatocellular carcinomas (HCC) (1). Successful treatment of chronic hepatitis C would reduce the morbidity and mortality of patients because around 8% of patients progressing to LC will develop HCC annually (2).

Spontaneous clearance following acute infection occurs in some cases for reasons that remain unclear, and previous studies report that 50% – 85% of patients progress to chronicity. The relationship between race and spontaneous viral clearance following acute infection have been reported (3 – 6). These characteristics based on ethnic types would suggest the effect of a host genetic factor on HCV infection.

*Corresponding author. ytanaka@med.nagoya-cu.ac.jp
Published online in J-STAGE on February 22, 2011 (in advance)
doi: 10.1254/jphs.10R15FM

2. HCV treatment and the response

The current standard of care for the HCV infections comprises pegylated interferon (PEG-IFN)-α 2a or 2b plus ribavirin (RBV). Successful treatment, termed "sustained virological response (SVR)", was defined by an HCV RNA negative after 6 months of completing therapy, whereas a transient viral response (TVR) was defined as a reappearance of HCV RNA in serum after treatment was discontinued in a patient who had undetectable HCV RNA during the therapy or on completion of the therapy (Fig. 1). A non-viral response (NVR) was defined as cases with detectable viremia after and during treatment. The standard therapy is effective in only 42% – 52% of patients with HCV genotype 1 in the US and Europe (7 – 9). A significant difference in response to PEG-IFN&RBV therapy between ethnicities were reported: the SVR achievement of African Americans was only approximately 20% – 28% compared to 40% – 52% in Caucasian patients with genotype 1 infection (10 – 12) and 57% vs. 82% for genotype 2/3 (13). The current therapies are limited by expensive, ineffectiveness in part of the patients, and numerous potentially severe side effects, which cause dose reduction and/or premature termination of treatment. Additionally, premature withdrawal from IFN-based therapy (14) was necessary for 10% – 14% of the patients, leading to failure of the HCV therapy.

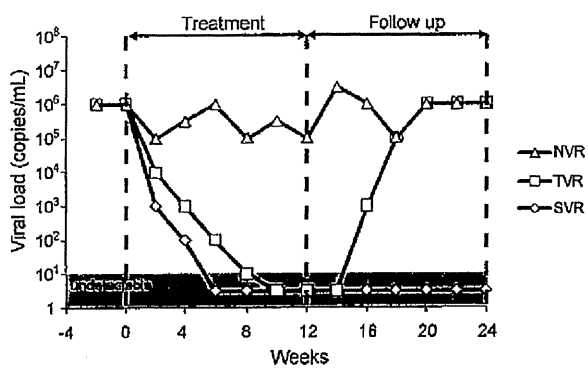

Fig. 1. Representative changes of HCV viral load in patients treated with PEG-IFN&RBV combination therapy. The response type under the therapy of PEG-IFN&RBV is divided into three groups: SVR, TVR, or NVR. SVR is defined as successful treatment, which is HCV RNA negative after 6 months of completing therapy. TVR is defined as a transiently negative for HCV RNA during treatment. However, after the end of therapy, HCV RNA of the patients reappears with impaired liver function in TVR. NVR is defined as a constitutive high viremia during and after treatment. SVR, sustained viral response; TVR, transient viral response; NVR, non-viral response

3. Viral factors associated with HCV therapy

To prevent treatment failure in such patients, we must identify the predictive factors leading to treatment failure as well as production of severe side effects in the clinic. Previous studies have reported that viral titer, mutations, or gene expression levels of innate immunity could be prediction factors for NVR using clinical specimens of chronic hepatitis C patients. Several viral factors such as genotype 1 (HCV-1), high baseline viral load, viral kinetics during treatment, and amino acid pattern in the IFN sensitivity–determining region have been found to be significantly associated with the outcome by a number of independent studies (15 – 17). Accumulated data have provided strong evidence that approximately 20% of patients with HCV genotype 1 have NVR to PEG-IFN&RBV. The reliable prediction for NVR would allow avoidance of side effects and reduce the cost of treatment in the 20% of patients with HCV-1 before starting the treatment.

4. Host factors associated with response to PEG-IFN&RBV therapy

Several host factors related to viral clearance have been reported based on clinical features or laboratory data, for example, gender, age <40 years, low HCV RNA level prior to treatment, lack of liver cirrhosis, and HCV genotypes 2/3 (18, 19). As for host genetic factor, candidate gene approaches have been adopted to identify host factors related to clinical outcomes, single nucleotides polymorphisms (SNPs), copy number variation (CNV), or insertion/deletion of genes. The approach could latently find weak associations and show significant differences because only one or a limited number of SNPs or gene loci are detected in candidate genes. The focused approach, however, contains the restraint to detect crucial factors. In detail, the selection of candidate regions for genetic study depends on the researcher's knowledge or the present data of the gene pathway.

In contrast, a recent genome-wide association study (GWAS) approach using high-throughput genotyping technology usually for SNPs, ranging from 300,000 to 900,000 SNPs in each sample, is able to detect strong association factors affecting disease susceptibility and drug response without any a-priori hypotheses on causative SNPs apart from the hypotheses (20, 21). On the basis of the GWAS, four independent groups assessed the role of genetic variation on response to PEG-IFN&RBV combination therapy for chronic hepatitis C patients, and the data was reported in a short-term (21 – 24). In all cases, the conclusive finding was that polymorphisms in or near the *IL-28B* gene strongly de-

termined the outcome of HCV therapy.

5. Study design of four studies for GWAS

Ge et al. and Suppiah et al. studied genetic variants associated with SVR to PEG-IFN&RBV therapy in individuals infected with HCV genotype 1 (21, 22). The former examined genetic factors associated with treatment response in patients from the IDEAL trial (Individualized Dosing Efficacy vs. flat dosing to Assess optimaL pegylated interferon therapy) (25), a large randomized controlled trial involving Caucasian, American-African, and Hispanic individuals in North America (n = 1137) (Table 1). The latter study group analyzed Caucasians consisting of 293 Australian individuals (Northern European ancestry) with HCV genotype 1 and also validates an independent replication cohort consisting of 555 Europeans from the UK, Germany, Italy, and Australia. These two study groups mainly investigated GWAS in Caucasians and analyzed host factors associated with SVR.

Tanaka et al. studied host factors associated with the response to PEG-IFN&RBV treatment in 142 Japanese patients with chronic hepatitis C of HCV genotype 1 for GWAS and prepared an independent replication cohort of 172 Japanese (Table 1) (24). In this study, patients were divided into three groups, SVR, TVR, or NVR. NVR vs. virological responder (VR) consisting of SVR and TVR was used for the predication of NVR factors. The data set of SVR vs. non-SVR (TVR and NVR) was constructed to discover the host factor related to SVR (Fig. 1).

Rauch et al. investigated 465 Caucasians infected with HCV genotypes 1, 2, 3, or 4 to reveal genetic variations associated with response to the combination therapy (23). A case control study was designed to detect genetic variations related to SVR in European individuals. Three study groups, except Suppiah et al., selected patients receiving at least 80% of the recommended treatment dose to emphasize genetic associations.

6. Identification of strongly significant SNPs associated with PEG-IFN&RBV therapy

Ge et al. identified a genetic polymorphism (rs12979860) near the *IL-28B* gene on chromosome 19, also known as IFN-λ3 (Fig. 2). Individuals with the CC genotype showed the association with an approximately two-fold change in response to PEG-IFN&RBV treatment compared with those with the TT genotype, both among patients of European ancestry ($P = 1.06 \times 10^{-25}$) and African-Americans ($P = 2.06 \times 10^{-3}$). An important finding in the study is the strong correlation between being a carrier of this SNP and SVR rates in diverse ethnic groups, which is significantly more frequent in European-Americans and Asian populations than in African-Americans. Approximately 23% – 55% of Africans (<40% of African-Americans) carry advantageous C-allele frequency of rs12979860, compared with approximately 53% – 85% of Europeans (<70% of European-

Table 1. Four GWAS groups studying host factor related to the response to HCV therapy

Study (Ref. No.)	Ge et al. (22)	Suppiah et al. (21)	Tanaka et al. (24)	Rauch et al. (23)
Region	Northern America	Northern Europe, Australia	Japan	Switzerland
Ancestry	Caucasian/ African/ Hispanic	Caucasian	Japanese	Caucasian
GWAS size	871/ 192/ 176	293	142	465
Replication	No replication	555	172	No replication
Case/control	SVR vs. non-SVR	SVR vs. non-SVR	SVR vs. non-SVR SVR&TVR vs. NVR	SVR vs. non-SVR
Adherence	Over 80% adherent to PEG-IFN&RBV during the first 12 weeks of therapy	Not controlled	Over 80% adherent to PEG-IFN&RBV during the first 12 weeks of therapy	Over 80% adherent to PEG-IFN&RBV during the first 12 weeks of therapy
HCV genotype	1	1	1	1, 2, 3, 4
Significant SNPs	rs12979860	rs8099917	rs8099917	rs8099917
P value	1.37×10^{-25}	9.25×10^{-5}	1.18×10^{-7}	3.11×10^{-8}
OR (95% CI)	3.1 (2.1 – 4.7)	1.98 (1.57 – 2.52)	12.1 (6.5 – 22.4)*	5.19 (2.9 – 9.3)
Platform	Illumina 610-quad	IlluminaCNV370-quad	Affymetrix SNP 6.0	Illumina Human 1M-duo Human Hap550 Human610W-quad

*The combined value in the study in comparison with SVR vs. non-SVR.

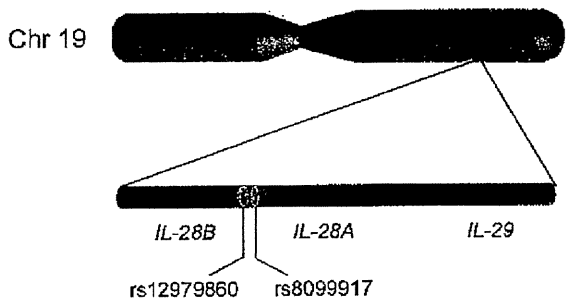

Fig. 2. *IL-28B* gene and SNPs location in chromosome 19. Four independent GWAS discovered SNPs strongly associated with the response to PEG-IFN&RBV therapy around *IL-28B* in chromosome 19. Ge et al. (22) reported rs12979860 as a strongly associated SNP, whereas Suppiah et al. (21), Tanaka et al. (24), and Rauch et al. (23) detected a statistical difference on rs8099917. These 2 SNPs are in strong linkage disequilibrium because these loci are very near to each other. The interferon lambda family consists of *IL-29* (IFN-λ1), *IL-28A* (IFN-λ2), and *IL-28B* (IFN-λ3), which are induced by type I IFN, or bacterial and viral infection.

Americans) and approximately 90% of Chinese and Japanese. Ge et al. showed that the SVR rates across different population groups displayed a striking concordance with the C-allele frequency. This SNP explained about half of the difference in response rates between African-Americans and Europeans.

Suppiah et al. and Tanaka et al. revealed the strong association of particular haplotypes of SNPs around *IL-28B* in the population of PEG-IFN&RBV therapy. The most significant SNPs in both study groups was rs8099917 (8 kb upstream of *IL-28B*) associated with SVR in European and Japanese patients (Fig. 2). Suppiah et al. also identified the association of rs8099917 in European ancestry with HCV genotype 1 based on the determination of SVR factors (combined $P = 9.25 \times 10^{-9}$, OR = 1.98, 95% CI = 1.57 – 2.52) (21). Homozygotes for the risk allele (rs8099917 G-allele) showed 2-fold higher risk of treatment failure than that of major allele homozygotes. In the gene expression assay, the minor allele of rs8099917 tended to suppress mRNA levels of *IL-28A/B*.

Tanaka et al. identified several SNPs significantly associated with NVR to PEG-IFN&RBV therapy in the GWAS and the replication study. All significant SNPs were located near the *IL-28B* locus on chromosome 19. The SNPs, rs12980275 or rs8099917, validated in an independent replication cohort showed the strongest association (combined $P = 2.84 \times 10^{-27}$ and 2.68×10^{-32}; OR = 17.7, 95% CI = 10.0 – 31.3; OR = 27.1, 95% CI = 14.6 – 50.3, respectively) (24). Interestingly, the minor alleles of the SNPs were accumulated in NVR (minor allele frequency of NVR = 74.3% for rs12980275 and 75.0% for rs8099917). Multivariate analyses containing genetic and clinical factors revealed that rs8099917 was the strongest predictor for response to therapy (P = 0.0001, OR = 37.68, 95% CI = 16.71 – 83.85).

The fourth GWAS was published on the response to HCV therapy, Rauch et al. studied patients infected with HCV genotype 1, 2, 3, or 4 (23). Rauch et al. also identified several SNPs around the *IL-28B* gene on chromosome 19 (Fig. 2). The strongest association with treatment failure was found with rs8099917 ($P = 3.11 \times 10^{-8}$, OR = 5.19). Interestingly, rs8099917 did not associate with the response to PEG-IFN&RBV therapy in genotype 2 or 3 patients. The contribution of host factors to genotype 2 or 3 clearance would be low because HCV genotype 2 or 3 is likely to be eliminated by the standard therapy compared with genotype 1. In individuals infected with HCV genotypes 1 and 4, the SVR rate of the patients harboring the minor allele was 28%, whereas that of the major allele homozygotes reached 63%. However, patients infected with genotypes 2 or 3 showed high viral response rate, approximately 80%, without statistical significance between the patients and the control.

7. The influence of genetic background on the statistical analysis

For the prediction of SVR, OR of the Japanese population was much higher than that of the other populations (Table 1). Individuals harboring the risk allele of rs8099917 or rs12979860 was approximately 10% in Asia, whereas the risk allele frequency was generally over 20% in European Caucasians. Moreover, individuals with the risk allele were the major population in individuals with African ancestry. The differences of allele frequency might explain, in part, the observed discrepancy in the response rate of viral clearance and the statistical power between racial groups.

Tanaka et al. extracted the data of TVR patients to analyze the genetic background. The minor allele frequency (MAF) of the strongly associated SNPs (rs8099917, located in the intergenic region between *IL-28A* and *IL-28B*) in TVR was similar to that of the SVR population (Fig. 3) (24). The statistical analysis for SVR prediction (SVR vs. non-SVR) using the SNPs showed lower statistical power (OR = 12.1) than that of NVR prediction (NVR vs. SVR plus TVR, OR = 27.1), indicating that the significant SNPs are strongly associated with the outcome of NVR. In other words, TVR patients share similar genetic background with SVR patients, and they would achieve SVR by prolonged therapy or PEG-IFN&RBV plus protease inhibitor.

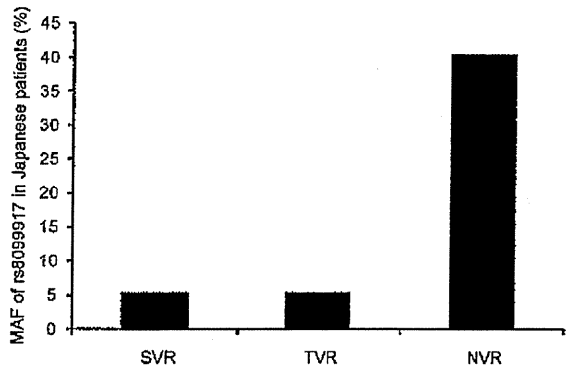

Fig. 3. Minor allele frequencies (MAF) of rs8099917 in each response type of chronic hepatitis C patients reported by Tanaka et al. (24). In the Asian population, the MAF of rs8099917 is approximately 10% according to Thomas et al. (20) and the dbSNPs international database. The MAF of chronic hepatitis C patients under a combination therapy of PEG-IFN&RBV revealed the deviation from that of the general population. The minor allele of rs8099917 accumulated in the population of NVR (approximately 40%), whereas those of SVR and TVR were occurred at lower frequency than those of the general population (approximately 5%).

8. SNPs associated with spontaneous clearance of HCV

Two study groups searched for common SNPs related to spontaneous elimination of HCV using a Caucasian cohort. Thomas et al. performed a candidate gene study on the rs12979860 SNP reported by Ge et al. to determine whether the SNP was also associated with spontaneous clearance of HCV infection (20). This study included 388 individuals with spontaneous HCV clearance and 620 with persistent HCV infection in a cohort consisting of HCV and HIV/HCV co-infected patients. The strong association of rs12979860 with spontaneous recovery was found in European and African American individuals (OR = 2.6, 95% CI = 1.9 – 3.8; OR = 3.1, 95% CI = 1.7 – 5.8, respectively) (Table 2). The association was also independent of co-infection with HIV, type of HCV transmission, and history of HBV infection.

Rauch et al. revealed the host factor associated with spontaneous clearance of HCV based on GWAS technology mounting more than 500K SNPs (23). The case-control study was designed for 347 individuals with spontaneous HCV clearance, 567 individuals with chronic hepatitis C, and 448 individuals with HCV/HIV co-infection. The significant SNP was also rs8099917 (combined $P = 6.07 \times 10^{-9}$, OR = 2.31, 95% CI = 1.74 – 3.04). The effect of HIV co-infection was also similar to that of HCV mono-infection ($P = 8.25 \times 10^{-5}$, OR = 2.16, 95% CI = 1.47 – 3.18; $P = 1.96 \times 10^{-5}$, OR = 2.49, 95% CI = 1.64 – 3.79, respectively) compared to Thomas et al. Note that rs8099917 was in strong linkage disequilibrium with rs12979860 in European and Asian individuals (26). These reports described by Thomas et al. and Rauch et al. seem to lead crucially identical results.

9. The characteristics of *IL-28B* and the IFN-λ family

IL-28B, referred to as IFN-λ3, belongs to the IFN-λ family, which consists of *IL-29*/IFN-λ1, *IL-28A*/IFN-λ2, and *IL-28B*. The *IL-28B* gene has been recently discovered and classified into type III IFN, a member of the class II cytokine family. This class II family includes type I, II, and III IFN and the *IL-10* family (*IL-10*, *IL-19*, *IL-20*, *IL-22*, *IL-24*, *IL-26*, *IL-28*, and *IL-29*). Peripheral blood mononuclear cells (PBMCs) and dendritic cells are main sources of IFN-λ (27, 28), which is induced by IFN-α, viral infection, and/or stimulations of toll-like receptors. IFN-λ behave as a interferon stimulated gene (ISG) of IFN-α, which is expressed at low levels by a broad variety of human cells, similar to IFN-α (29).

The signal pathway of IFN-λ is initiated through a membrane receptor distinct from that of type I IFN. The receptor is composed of heterodimer molecules consisting of an IL-28RA/IFN-λR1 subunit and IL-10R2 subunit (27, 28). The IL-10R2 subunit is expressed broadly and shared by IL-10, IL-22, IL-26, and IFN-λ. Compared with the IFN-α /-β receptor, which is ubiquitously expressed, the IL-28RA receptor has a more restricted distribution. The signal transduction of IFN-λ receptor is mediated via Jak1 and Tyk2, which can induce the phos-

Table 2. Summary of associated SNPs regarding spontaneous clearance of HCV

Study (Ref. No.)	Thomas et al. (20)		Rauch et al. (23)		
SNPs	rs12979860		rs8099917		
Population	European	African	HCV mono-infection	HCV/HIV co-infection	Combined
P value	1.0×10^{-7}	1.0×10^{-4}	1.96×10^{-5}	8.25×10^{-5}	6.07×10^{-9}
OR	2.6	3.1	2.49	2.16	2.31
95% CI	1.85 – 3.84	1.75 – 5.88	1.64 – 3.79	1.47 – 3.18	1.74 – 3.04

phorylation of STAT1 and STAT2 molecules and is followed by the expression of ISG (30).

10. The antiviral effect of IFN-λ against HCV in basic studies or clinical trials

Antiviral effects of IFN-λs against HCV have been reported before the discovery of the association with the response to HCV therapy. The treatment of IFN-α, or IFN-λ1 inhibited HCV replication at similar levels at low concentrations (31). The combination treatment of IFN-α and *IL-29/28A* enhanced the antiviral effect against HCV replicon synergistically (32). In microarray analysis on ISG induction of IFN-α/β or IFN-λ1, IFN-λ1 showed a unique pattern of ISG expression compared to that of IFN-α/β (31). For example, a total of 19 genes, which were not detected in the IFN-α–treated cells, were specifically up-regulated by IFN-λ1 at the late phase of treatment, indicating the signal pathway downstream of IL-28R1 could differ from that of IFN-α and possess a important biological function, although the pattern of signal transduction currently thought to be similar to that of IFN-α R1/2 (33). Further studies are needed to elucidate the biological consequences of these differences.

As described above, HCV replication is inhibited by the antiviral effects of IFN-λ. IFN-λ might have potential as a therapeutic agent against chronic hepatitis C in patients. A pegylated IFN-λ1 has already been tried against chronic hepatitis C in phase 1B trials (34). Interestingly, sufficient antiviral effects were observed but not severe side effects. The expression pattern of the IFN-λ receptor is restricted in specific organs. The high expression of the receptor was observed in the pancreas, liver, prostate, or thyroid, whereas the central nerve system (the bone marrow or the brain) showed the low expression (27, 28). These results could explain the avoidance of severe toxicity induced by IFN-α/β.

11. Conclusions

The recent discovery revealed by GWAS technology provides the unexpected role of *IL-28B* in HCV infection. The findings could be strong evidence to enhance the development of a novel therapeutic strategy and basic studies on IFN-λs. The SNPs around the *IL-28B* gene could improve the diagnostics for the prediction of spontaneous clearance and the response to anti-HCV treatment. However, approximately 20% – 30% of the total homozygotes with the risk alleles in Caucasians and 20% of heterozygotes/homozygotes with risk alleles in the Japanese population achieved a SVR and vice versa (21 – 24), indicating that the response to a combination therapy is not inevitably restricted because of genetic factors. To improve the prediction rate, especially, host epigenetic, rare SNPs, mutations, or viral factors are eligible candidates to consider when trying to establish an adequate tailor-made therapy. Although the strongly associated SNPs may have a big impact on the type of therapy and outcome, this is the first step in the tailor-made therapy for HCV infection. Further functional studies of IFN-λs and the significant SNPs should be investigated to improve the positive predictive value using the point mutation analysis of the targeted polymorphisms (35). For applying a practical tailor-made therapy, it is also necessary to reveal the cause of exceptional cases that do not follow the *IL-28B* genotyping.

References

1 Hoofnagle JH. Course and outcome of hepatitis C. Hepatology. 2002;36:S21–S29.

2 Shiratori Y, Shiina S, Imamura M, Kato N, Kanai F, Okudaira T, et al. Characteristic difference of hepatocellular carcinoma between hepatitis B- and C-viral infection in Japan. Hepatology. 1995;22:1027–1033.

3 Grebely J, Raffa JD, Lai C, Krajden M, Conway B, Tyndall MW. Factors associated with spontaneous clearance of hepatitis C virus among illicit drug users. Can J Gastroenterol. 2007;21: 447–451.

4 Thomas DL, Astemborski J, Rai RM, Anania FA, Schaeffer M, Galai N, et al. The natural history of hepatitis C virus infection: host, viral, and environmental factors. Jama. 2000;284:450–456.

5 Aborsangaya KB, Dembinski I, Khatkar S, Alphonse MP, Nickerson P, Rempel JD. Impact of aboriginal ethnicity on HCV core-induced IL-10 synthesis: interaction with IL-10 gene polymorphisms. Hepatology. 2007;45:623–630.

6 Busch MP, Glynn SA, Stramer SL, Orland J, Murphy EL, Wright DJ, et al. Correlates of hepatitis C virus (HCV) RNA negativity among HCV-seropositive blood donors. Transfusion. 2006;46: 469–475.

7 Fried MW, Shiffman ML, Reddy KR, Smith C, Marinos G, Goncales FL Jr, et al. Peginterferon alfa-2a plus ribavirin for chronic hepatitis C virus infection. N Engl J Med. 2002;347: 975–982.

8 Hadziyannis SJ, Sette H Jr, Morgan TR, Balan V, Diago M, Marcellin P, et al. Peginterferon-alpha2a and ribavirin combination therapy in chronic hepatitis C: a randomized study of treatment duration and ribavirin dose. Ann Intern Med. 2004;140: 346–355.

9 Manns MP, McHutchison JG, Gordon SC, Rustgi VK, Shiffman M, Reindollar R, et al. Peginterferon alfa-2b plus ribavirin compared with interferon alfa-2b plus ribavirin for initial treatment of chronic hepatitis C: a randomised trial. Lancet. 2001;358: 958–965.

10 Conjeevaram HS, Fried MW, Jeffers LJ, Terrault NA, Wiley-Lucas TE, Afdhal N, et al. Peginterferon and ribavirin treatment in African American and Caucasian American patients with hepatitis C genotype 1. Gastroenterology. 2006;131:470–477.

11 Jeffers LJ, Cassidy W, Howell CD, Hu S, Reddy KR. Peginterferon alfa-2a (40 kd) and ribavirin for black American patients with chronic HCV genotype 1. Hepatology. 2004;39:1702–1708.

12 Muir AJ, Bornstein JD, Killenberg PG. Peginterferon alfa-2b and ribavirin for the treatment of chronic hepatitis C in blacks and non-Hispanic whites. N Engl J Med. 2004;350:2265–2271.
13 Shiffman ML, Mihas AA, Millwala F, Sterling RK, Luketic VA, Stravitz RT, et al. Treatment of chronic hepatitis C virus in African Americans with genotypes 2 and 3. Am J Gastroenterol. 2007;102:761–766.
14 Fried MW. Side effects of therapy of hepatitis C and their management. Hepatology. 2002;36:S237–S244.
15 Akuta N, Suzuki F, Sezaki H, Suzuki Y, Hosaka T, Someya T, et al. Association of amino acid substitution pattern in core protein of hepatitis C virus genotype 1b high viral load and non-virological response to interferon-ribavirin combination therapy. Intervirology. 2005;48:372–380.
16 Pascu M, Martus P, Hohne M, Wiedenmann B, Hopf U, Schreier E, et al. Sustained virological response in hepatitis C virus type 1b infected patients is predicted by the number of mutations within the NS5A-ISDR: a meta-analysis focused on geographical differences. Gut. 2004;53:1345–1351.
17 Shirakawa H, Matsumoto A, Joshita S, Komatsu M, Tanaka N, Umemura T, et al. Pretreatment prediction of virological response to peginterferon plus ribavirin therapy in chronic hepatitis C patients using viral and host factors. Hepatology. 2008;48:1753–1760.
18 Walsh MJ, Jonsson JR, Richardson MM, Lipka GM, Purdie DM, Clouston AD, et al. Non-response to antiviral therapy is associated with obesity and increased hepatic expression of suppressor of cytokine signalling 3 (SOCS-3) in patients with chronic hepatitis C, viral genotype 1. Gut. 2006;55:529–535.
19 Gao B, Hong F, Radaeva S. Host factors and failure of interferon-alpha treatment in hepatitis C virus. Hepatology. 2004;39:880–890.
20 Thomas DL, Thio CL, Martin MP, Qi Y, Ge D, O'Huigin C, et al. Genetic variation in IL28B and spontaneous clearance of hepatitis C virus. Nature. 2009;461:798–801.
21 Suppiah V, Moldovan M, Ahlenstiel G, Berg T, Weltman M, Abate ML, et al. IL28B is associated with response to chronic hepatitis C interferon-alpha and ribavirin therapy. Nat Genet. 2009;41:1100–1104.
22 Ge D, Fellay J, Thompson AJ, Simon JS, Shianna KV, Urban TJ, et al. Genetic variation in IL28B predicts hepatitis C treatment-induced viral clearance. Nature. 2009;461:399–401.
23 Rauch A, Kutalik Z, Descombes P, Cai T, Di Iulio J, Mueller T, et al. Genetic variation in IL28B is associated with chronic hepatitis C and treatment failure: a genome-wide association study. Gastroenterology. 2010;138:1338–1345, 1345.e1331–e1337.
24 Tanaka Y, Nishida N, Sugiyama M, Kurosaki M, Matsuura K, Sakamoto N, et al. Genome-wide association of IL28B with response to pegylated interferon-alpha and ribavirin therapy for chronic hepatitis C. Nat Genet. 2009;41:1105–1109.
25 McHutchison JG, Lawitz EJ, Shiffman ML, Muir AJ, Galler GW, McCone J, et al. Peginterferon alfa-2b or alfa-2a with ribavirin for treatment of hepatitis C infection. N Engl J Med. 2009;361:580–593.
26 Tanaka Y, Nishida N, Sugiyama M, Tokunaga K, Mizokami M. lambda-Interferons and the single nucleotide polymorphisms: A milestone to tailor-made therapy for chronic hepatitis C. Hepatol Res. 2010;40:449–460.
27 Kotenko SV, Gallagher G, Baurin VV, Lewis-Antes A, Shen M, Shah NK, et al. IFN-lambdas mediate antiviral protection through a distinct class II cytokine receptor complex. Nat Immunol. 2003;4:69–77.
28 Sheppard P, Kindsvogel W, Xu W, Henderson K, Schlutsmeyer S, Whitmore TE, et al. IL-28, IL-29 and their class II cytokine receptor IL-28R. Nat Immunol. 2003;4:63–68.
29 Siren J, Pirhonen J, Julkunen I, Matikainen S. IFN-alpha regulates TLR-dependent gene expression of IFN-alpha, IFN-beta, IL-28, and IL-29. J Immunol. 2005;174:1932–1937.
30 Donnelly RP, Sheikh F, Kotenko SV, Dickensheets H. The expanded family of class II cytokines that share the IL-10 receptor-2 (IL-10R2) chain. J Leukoc Biol. 2004;76:314–321.
31 Marcello T, Grakoui A, Barba-Spaeth G, Machlin ES, Kotenko SV, MacDonald MR, et al. Interferons alpha and lambda inhibit hepatitis C virus replication with distinct signal transduction and gene regulation kinetics. Gastroenterology. 2006;131:1887–1898.
32 Brand S, Zitzmann K, Dambacher J, Beigel F, Olszak T, Vlotides G, et al. SOCS-1 inhibits expression of the antiviral proteins 2',5'-OAS and MxA induced by the novel interferon-lambdas IL-28A and IL-29. Biochem Biophys Res Commun. 2005;331:543–548.
33 O'Brien TR. Interferon-alfa, interferon-lambda and hepatitis C. Nat Genet 2009;41:1048–1050.
34 Muir AJ, Shiffman ML, Zaman A, Yoffe B, de la Torre A, Flamm S, et al. Phase 1b study of pegylated interferon lambda 1 with or without ribavirin in patients with chronic genotype 1 hepatitis C virus infection. Hepatology. 2010;52:822–832.
35 Sakata T, Anzai N, Kimura T, Miura D, Fukutomi T, Takeda M, et al. Functional analysis of human organic cation transporter OCT3 (SLC22A3) polymorphisms. J Pharmacol Sci. 2010;113:263–266.

EMBO reports

scientific report

Protein phosphatase 1γ is responsible for dephosphorylation of histone H3 at Thr 11 after DNA damage

Midori Shimada[1], *Mayumi Haruta*[1], *Hiroyuki Niida*[1], *Kazunobu Sawamoto*[2] & *Makoto Nakanishi*[1+]
[1]Department of Cell Biology, and [2]Developmental and Regenerative Biology, Graduate School of Medical Sciences, Nagoya City University, Nagoya, Japan

The DNA-damage-induced transcriptional suppression of cell cycle regulatory genes correlates with a reduction in histone H3-Thr 11 phosphorylation (H3-pThr 11) on their promoters that is partly mediated by the dissociation of Chk1 from chromatin. In this study, we identify protein phosphatase 1γ (PP1γ) as a phosphatase responsible for DNA-damage-induced H3-pThr 11 dephosphorylation. PP1γ is activated after DNA damage, which is mainly mediated by a reduction in Cdk-dependent phosphorylation of PP1γ at Thr 311. The depletion of PP1γ sensitizes HCT116 cells to DNA damage. Our results suggest that the ataxia telangiectasia, mutated and Rad3-related–Chk1 axis regulates H3-pThr 11 dephosphorylation on DNA damage, at least in part by the activation of PP1γ through Chk1-dependent inhibition of Cdks.

Keywords: PP1; DNA damage; transcription; checkpoint; Cdk
EMBO *reports* (2010) 11, 883–889. doi:10.1038/embor.2010.152

INTRODUCTION

Eukaryotic cells have coordinated systems to respond to DNA damage, such as cell cycle arrest mechanisms, DNA repair pathways and the apoptotic response. Together, these maintain genomic integrity (Sancar *et al*, 2004). These systems are partly regulated by transcriptional activation and repression (Zhan *et al*, 1993; Engelberg *et al*, 1994). We and others have recently identified histone H3-Thr 11 phosphorylation (H3-pThr 11) as a new transcriptional marker (Metzger *et al*, 2008; Shimada & Nakanishi, 2008; Shimada *et al*, 2008) that rapidly decreases after DNA damage. Under normal conditions Chk1 associates with chromatin (Smits *et al*, 2006; Niida *et al*, 2007) and phosphorylates H3-Thr 11. In response to DNA damage, Chk1 is rapidly released from chromatin and H3-pThr 11 is reduced.

[1]Department of Cell Biology, and
[2]Developmental and Regenerative Biology, Graduate School of Medical Sciences, Nagoya City University, 1 Kawasumi, Mizuho-cho, Mizuho-ku, Nagoya 467-8601, Japan
+Corresponding author. Tel: +81 52 853 8144; Fax: +81 52 842 3955; E-mail: mkt-naka@med.nagoya-cu.ac.jp

Received 29 April 2010; revised 31 August 2010; accepted 31 August 2010; published online 15 October 2010

Mammalian serine (Ser)/threonine (Thr)-specific protein phosphatases (PPs) are represented by eight distinct prototypes: PP1, PP2A, PP2B, PP2C, PP4, PP5, PP6 and PP7 (Moorhead *et al*, 2007; Swingle *et al*, 2007). Of these, PP1, PP2A and PP4 have all been identified as histone phosphatases: PP1 dephosphorylates H1, which is phosphorylated in a cell-cycle-dependent manner (Paulson *et al*, 1996). The PP1 homologue dephosphorylates H3-pSer 10 at mitotic exit in yeast and worms (Hsu *et al*, 2000), and PP2A contributes to its dephosphorylation in *Drosophila* (Nowak *et al*, 2003). Phospho-H2AX (γ-H2AX) is immediately dephosphorylated after DNA repair by PP2A and PP4 in mammals and yeasts (Chowdhury *et al*, 2005, 2008; Keogh *et al*, 2006; Nakada *et al*, 2008). However, the phosphatases that catalyse H3-pThr 11 dephosphorylation in response to DNA damage have yet to be identified. In this study, we identify PP1γ as a phosphatase responsible for DNA-damage-induced dephosphorylation of H3-pThr 11.

RESULTS AND DISCUSSION

Dephosphorylation of pThr 11 is okadaic acid sensitive

To identify phosphatases that might be capable of DNA-damage-induced dephosphorylation of H3-pThr 11, we treated HeLa cells with different concentrations of okadaic acid (OA) and examined the status of H3-pThr 11 after ultraviolet (UV) irradiation. H3-pThr 11 was reduced after UV irradiation as previously reported (Shimada *et al*, 2008). Treatment with ⩾25 nM OA resulted in an increase in H3-pThr 11 in the absence of UV, making it difficult to evaluate the effect of OA treatment on DNA-damage-induced dephosphorylation of H3-pThr 11 (Fig 1A). We have previously reported that H3-pThr 11 is strongly enhanced at mitosis (Shimada *et al*, 2008). To establish whether the induction of H3-pThr 11 on OA treatment simply reflected an increase in the number of mitotic cells, we stained OA-treated cells with 4′,6-diamidino-2-phenylindole (DAPI) and calculated the mitotic index (Fig 1B). The mitotic index value increased more than threefold after OA treatment. However, in interphase cells, H3-pThr 11 is detected throughout the nuclear region with some exclusion of the peri-centromeric heterochromatin foci (represented by DAPI foci in Fig 1C). By contrast, at mitosis, strong

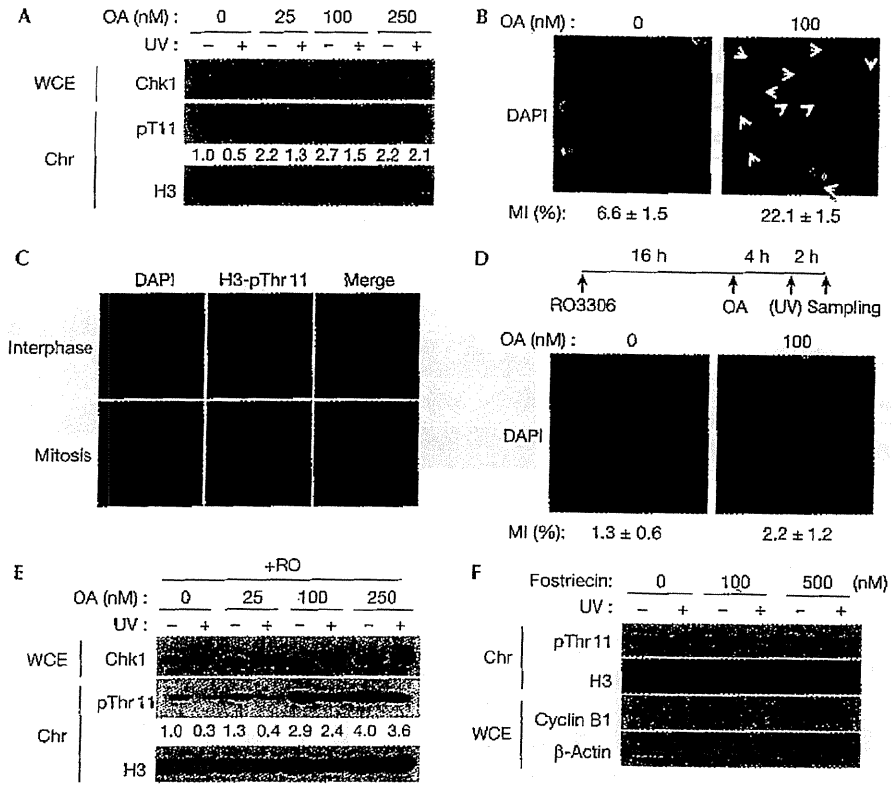

Fig 1 | The phosphatase responsible for H3-pThr11 dephosphorylation is sensitive to okadaic acid. (A) HeLa cells were pre-treated with the indicated concentrations of OA for 4 h. After irradiation with (+) or without (−) 100 J/m² UV, cells were cultured for an additional 2 h in the medium containing OA. WCE and Chr fractions were subjected to immunoblotting using the indicated antibodies. H3-pThr11 was quantified using NIH Image 1.62 Software and normalized relative to the total H3. The results were expressed at the bottom of the second panel as relative levels of H3-pThr11 compared with non-treated samples (0 h). (B) HeLa cells were fixed after the 6 h incubation with the indicated concentrations of OA and were stained with DAPI. The mitotic index (MI) indicates the percentage of cells with condensed chromosomes. Data are shown as means ± s.d. of four independent experiments. White arrowheads indicate mitotic cells. (C) MEFs were double-stained with H3-pThr11 antibodies and DAPI. Typical staining patterns of H3-pThr11 at interphase and mitosis are shown. (D) A scheme of the experimental strategy using HeLa cells and the MIs expressed as in (B) are shown. RO3306, 9 μM; OA, 100 nM. (E) HeLa cells irradiated with UV according to the strategy shown in (D) were collected, and WCE and Chr fractions were analysed by immunoblotting using the indicated antibodies. H3-pThr11 was quantified as in (A) and the results are shown at the bottom of the second panel. (F) HeLa cells incubated with fostriecin for 48 h were treated with (+) or without (−) UV. After 2 h incubation, WCE and chromatin fractions were subjected to immunoblotting. Chr, chromatin; DAPI, 4′,6-diamidino-2-phenylindole; MEF, mouse embryonic fibroblast; MI, mitotic index; NIH, National Institutes of Health; OA, okadaic acid; UV, ultraviolet; WCE, whole-cell extracts.

signals for H3-pThr11 are detected in condensed chromosomes, as reported previously (Preuss *et al*, 2003).

To evaluate the precise effect of OA treatment on H3-pThr11 independent of mitotic entry, we concomitantly treated cells with RO3306. Treatment with 9 μM RO3306 preferentially inhibits Cdk1 and thus prevents mitotic entry (Vassilev *et al*, 2006). The OA treatment did not result in an increase in the number of mitotic cells in the presence of 9 μM RO3306 (Fig 1D). Cell cycle arrest at G2 phase was induced as expected (supplementary Fig S1 online). DNA-damage-induced H3-pThr11 dephosphorylation was obvious at <100 nM OA, but almost completely abrogated at ≧100 nM OA in the presence of RO3306 when bands responsible for H3-pThr11 were quantified (Fig 1E). We observed that dephosphorylation of H3-pThr11 was not reduced after DNA damage, even at concentrations of 500 nM fostriecin—a specific inhibitor of PP2A—and its closely related PP4 and PP6 isotypes (Walsh *et al*, 1997; Fig 1F). At 100 nM, cyclin B1 had accumulated, demonstrating that inhibition was effective (Cheng *et al*, 1998). These results suggest that PP2A and its related phosphatases are not involved in DNA-damage-induced dephosphorylation of H3-pThr11.

PP1γ is a H3-pThr11 phosphatase

The OA sensitivity and fostriecin insensitivity in DNA-damage-induced dephosphorylation of H3-pThr11 suggested that the corresponding phosphatase might be a PP1 family member. We depleted PP1 by the using small interfering RNA (siRNA) that could suppress the expression of all three isoforms (PP1α, PP1β/δ and PP1γ) equally. Cells were treated with control, PP1 or PP2A siRNAs for 36 h in the presence of 0.5 mM hydroxyurea,

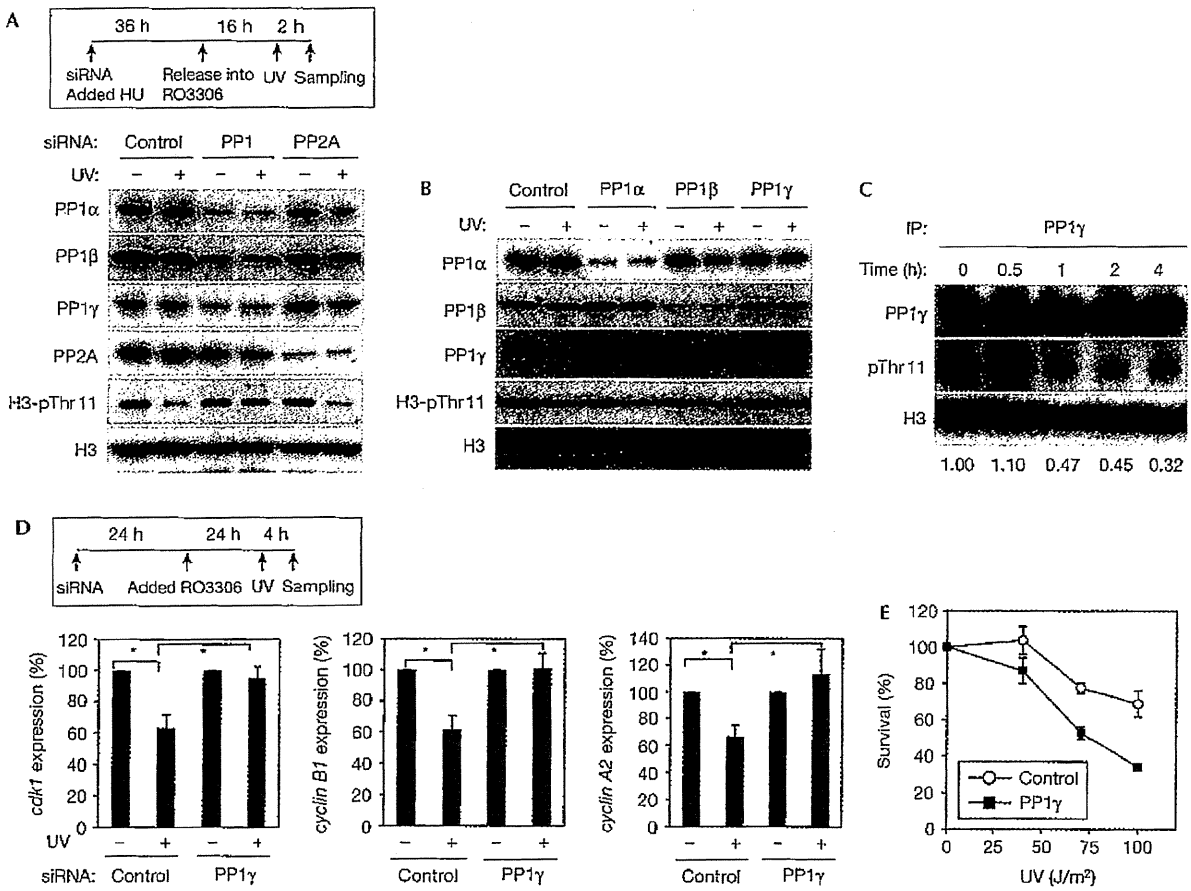

Fig 2 | Protein phosphatase 1γ is responsible for DNA-damage-induced dephosphorylation of H3-pThr11. (A) The experimental strategy is shown (upper panel). Whole-cell extracts with (+) or without (−) 100 J/m² UV were subjected to immunoblotting. (B) HCT116 cells were transfected with control, PP1 or PP2A siRNAs. After 70 h, cells were treated with (+) or without (−) 100 J/m² UV. After 2 h incubation, cells were collected and whole-cell extracts were subjected to immunoblotting. (C) MEFs were exposed to UV (100 J/m²) irradiation and collected at the indicated times. Endogenous PP1γ on the chromatin fraction was immunoprecipiated and the precipitates were subjected to immunoblotting and to an *in vitro* phosphatase assay using chromatin as a substrate. Phosphatase activity was examined by using immunoblotting with H3-pThr11 antibodies. H3-pThr11 was quantified and normalized relative to the total H3 as described in Fig 1E. The results are expressed as relative levels of H3-pThr11 compared with non-treated samples (0 h). (D) The experimental strategy is shown (upper panel). Total RNAs were prepared from HCT116 cells and quantitative real-time RT–PCR was performed using a set of primers within *cdk1, cyclin B1 and cyclin A2* transcripts. *$P<0.003$. (E) HCT116 cells transfected with control or PP1γ siRNAs for 72 h in 96-well plates were irradiated with UV (0, 40, 70 and 100 J/m²). The cell viability was determined 72 h after UV by MTT assay as described in the Methods section. The results were expressed as the percentage ratio of non-irradiated cells. MEF, mouse embryonic fibroblast; MTT, 3-(4,5-dimethylthiazol-2-yl)-2,5-diphenyltetrazolium bromide; PP, protein phosphatase; RT–PCR, reverse transcriptase PCR; siRNA, small interfering RNA; UV, ultraviolet.

which prevents mitotic arrest by PP1 or PP2A depletion. After 36 h, cells were released from hydroxyurea arrest and incubated with RO3306 for 16 h. Finally, cells were irradiated with UV and sampled 2 h later (Fig 2A, upper panel). The depletion of PP1, but not of PP2A, resulted in compromised H3-pThr11 dephosphorylation after UV (Fig 2A).

We further demonstrated that PP1γ depletion specifically compromised DNA-damage-induced H3-pThr11 dephosphorylation in both HCT116 (Fig 2B) and HeLa (supplementary Fig S2A,B online) cells. Depletion of individual PP1 subunits did not result in gross changes in cell cycle distribution, although PP1γ depletion mitotic index resulted in a slight increase in the mitotic index value (supplementary Fig S3 online). It is interesting to note that PP1γ phosphatase activity towards H3-pThr11 was activated as early as 1 h and maintained for up to 4 h after DNA damage (Fig 2C). Changes in the expression of cell cycle regulatory genes after PP1γ depletion were examined in cells treated with RO3306 to prevent low-level induction of mitotic cells. Treatment with RO3306 did not affect the expression of these genes (supplementary Table S1 online). The depletion of PP1γ suppressed DNA-damage-induced transcriptional repression of *cdk1, cyclin B1* and *cyclin A2* (Fig 2D). Importantly, PP1γ depletion sensitized HCT 116 cells to UV when cell survival was evaluated by MTT (3-[4,5-dimethylthiazol-2-yl]-2,5-diphenyltetrazolium bromide)

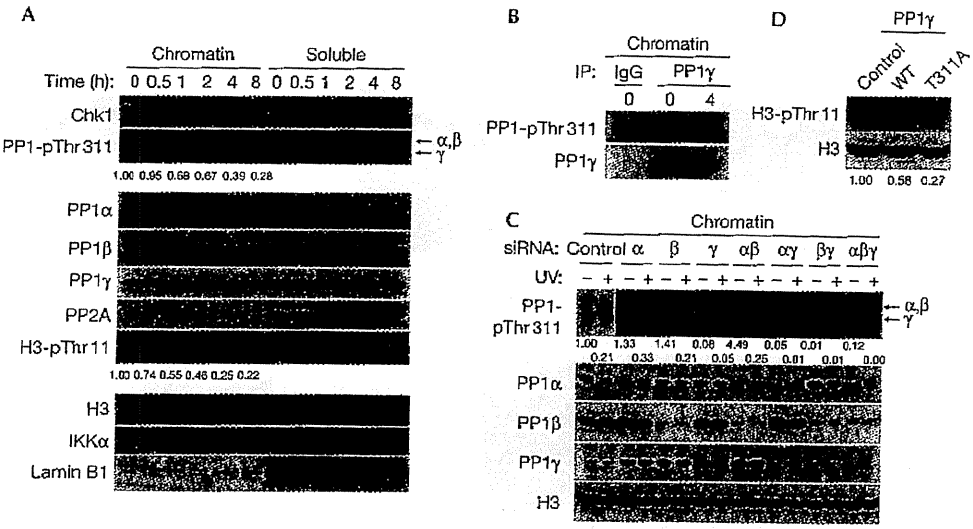

Fig 3 | Protein phosphatase 1γ-pThr311 on chromatin is decreased after DNA damage. (A) HCT116 cells were treated with UV (100 J/m²) and collected at the indicated times. The chromatin and soluble fractions were subjected to immunoblotting using the indicated antibodies. IKKα and lamin B1 were used as markers of soluble proteins. PP1γ-pThr311 and H3-pThr11 were quantified and normalized relative to the total PP1γ and H3, respective. The results are expressed at the bottom of the second and seventh panels as relative levels of PP1γ-pThr311 and H3-pThr11 compared with non-treated samples (0 h). (B) Chromatin fractions from UV-irradiated HCT116 cells were solubilized and subjected to IP-western analysis using the indicated antibodies. (C) To separate the isoforms of PP1 by SDS–PAGE, chromatin fractions from cells depleted of the indicated PP1 isoforms with (+) or without (−) UV were subjected to immunoblotting using an SDS–PAGE gel containing 10 μM Phos Tag. Arrows indicate bands corresponding to PP1α, β and γ isoforms. PP1γ-pThr311 was quantified and the results were expressed at the bottom of the first panel as relative levels of PP1γ-pThr311 compared with control (−UV). (D) The wild type or the T311A mutant of His-PP1γ purified from Sf9 cells were incubated with chromatin from HCT116 cells for 1 h at 30 °C. The status of H3-pThr11 was monitored by immunoblotting using H3-pThr11 antibodies. H3-pThr11 was quantified and normalized relative to the total H3. The results are expressed at the bottom of the second panel as relative levels of H3-pThr11 compared with the control sample. IKKα, IkB kinase α; IP, immunoprecipitation; PP, protein phosphatase; SDS–PAGE, sodium dodecyl sulphate–polyacrylamide gel electrophoresis; UV, ultraviolet.

assay (Fig 2E), suggesting the physiological importance of PP1γ-dependent transcriptional repression after DNA damage. Although the molecular mechanism by which PP1γ regulates H3-pThr11 dephosphorylation after DNA damage has remained elusive, isoform-specific functions for PP1 have been reported in the regulation of SRp38 dephosphorylation (Shi & Manley, 2007) and in the control of chromosomal architecture (Trinkle-Mulcahy *et al*, 2006).

Regulation of PP1γ activity in response to DNA damage

The activity of PP1α is reported to be downregulated by Cdk-dependent Thr320 phosphorylation (Dohadwala *et al*, 1994). The equivalent threonine residue is conserved in all three PP1 isoforms (Thr316 in PP1β/δ and Thr311 in PP1γ). Indeed, cyclin B1–Cdk1-phosphorylated PP1γ-Thr311 *in vitro* (supplementary Fig S4A online). Cdk activity is strongly inhibited after DNA damage, in a manner dependent on Chk1 (Harper & Elledge, 2007). We therefore examined changes in the phosphorylation status of PP1 subunits after UV irradiation by using a combination of isoform-specific antibodies and a phospho-specific Thr320 (PP1α) antibody (Fig 3A). All PP1 isoforms were similarly localized in both chromatin and soluble fractions of HCT116 cells. As a control, IkB kinase α (IKKα)—a typical cytosolic protein—and lamin B1—a marker of the nuclear soluble fraction—were predominantly detected in the soluble fraction, indicating that the subcellular fractionation was successful. The PP1-pThr320-specific signal for each isoform was rapidly dephosphorylated in response to UV, particularly in the chromatin fraction, with kinetics that were similar to that of H3-pThr11. As the PP1α-pThr320-specific antibody can recognize the corresponding phosphorylations of PP1β/δ and PP1γ, we further examined whether PP1γ-pThr311 was dephosphorylated after UV treatment. We observed that PP1γ-pThr311 in PP1γ immune complexes was reduced (Fig 3B). We separated the three isoforms of PP1 using sodium dodecyl sulphate–polyacrylamide gel electrophoresis containing Phos Tag (Kinoshita *et al*, 2009). Treatment of HCT116 cells with each isoform-specific siRNA or their combinations revealed that PP1γ migrated fastest, followed by PP1α and PP1β (Fig 3C), although the amounts of each isoform and their phosphorylations at Thr311 were induced after depletion of the other isoforms, presumably due to a compensatory mechanism. The PP1γ-pThr311-specific signal was consistently decreased in response to UV irradiation when bands responsible for PP1γ-pThr311 were quantified. Similar kinetics were observed when cells were treated with bleomycin (supplementary Fig S4B online) or ionizing radiation (supplementary Fig S4C online), and the extent of PP1γ-pThr311 dephosphorylation was found to be dependent on the UV dose (supplementary Fig S4D online). Importantly, the phosphorylation-defective mutant of PP1γ (T311A) was more active *in vitro* than in the wild-type PP1γ (Fig 3D).

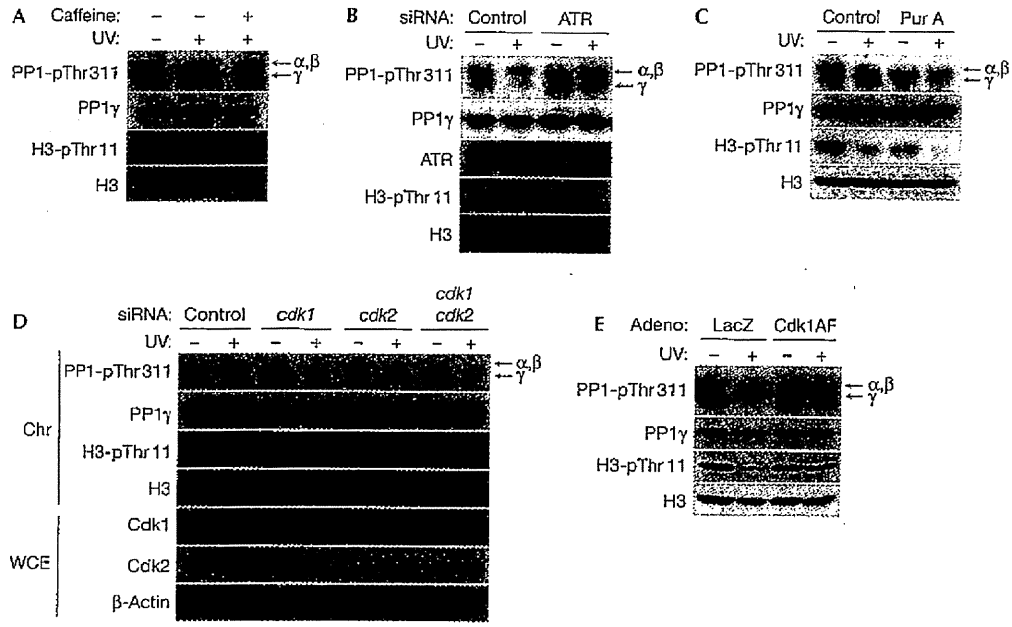

Fig 4 | Cdk-dependent phosphorylation of protein phosphatase 1γ at Thr311 is involved in DNA-damage-induced transcriptional repression. (A) HCT116 cells were pre-incubated in the presence (+) or absence (−) of 5 mM caffeine for 4 h and then treated with (+) or without (−) UV (100 J/m²). Cells were collected 2 h after UV treatment and their chromatin fractions were analysed by immunoblotting using the indicated antibodies. (B) HCT116 cells were transfected with control or ATR siRNAs. After 70 h, cells were treated with (+) or without (−) UV (100 J/m²) and incubated for an additional 4 h. Chromatin fractions were analysed by immunoblotting. (C) HCT116 cells were treated with 10 μM purvalanol A for 22 h, irradiated with UV (100 J/m²) and incubated for an additional 4 h. The chromatin fractions were analysed by immunoblotting. (D) HCT116 cells were transfected with control, *cdk1* and/or *cdk2* siRNAs. After 70 h, cells were treated with (+) or without (−) UV (100 J/m²) and incubated for an additional 4 h. The chromatin fractions or WCE were analysed by immunoblotting using the indicated antibodies. (E) HCT116 cells were infected with adenoviruses expressing LacZ as a control or the constitutively active Cdk1 mutant (Cdk1AF), and treated with (+) or without (−) UV (100 J/m²) 24 h after infection. Cells were collected 4 h after UV treatment and their chromatin fractions were analysed by immunoblotting using the indicated antibodies. ATR, ataxia telangiectasia, mutated and Rad3-related; Chr, chromatin; PP, protein phosphatase; siRNA, small interfering RNA; UV, ultraviolet; WCE, whole-cell extracts.

ATR–Chk1 axis regulates PP1γ activity

Treatment with caffeine—an inhibitor of the ataxia telangiectasia, mutated and Rad3-related (ATR) and ataxia telangiectasia, mutated kinases—partly suppressed DNA-damage-dependent dephosphorylation of PP1γ-pThr311 (Fig 4A). The knockdown of ATR by siRNA compromised UV-dependent PP1γ-pThr311 dephosphorylation (Fig 4B). Treatment with purvalanol A, a specific Cdk inhibitor, resulted in almost complete reduction in PP1γ-pThr311 and H3-pThr11 in the absence of DNA damage (Fig 4C). Both PP1γ-pThr311 and H3-pThr11 were significantly reduced when Cdk1 was depleted, and further reduced when both Cdk1 and Cdk2 were depleted (Fig 4D). By contrast, ectopic expression of a constitutively active Cdk1 mutant (Cdk1AF) inhibited UV-induced dephosphorylation of PP1γ-pThr311 and H3-pThr11 (Fig 4E). These results suggest that ATR/Chk1-dependent inhibition of Cdk activity results in dephosphorylation of PP1γ-pThr311 and activation of PP1γ, leading to dephosphorylation of H3-pThr11 (Fig 5).

In this study, we demonstrate that the dephosphorylation of H3-pThr11 and the subsequent transcriptional repression of cell cycle regulatory genes after DNA damage are regulated at least in part by the ATR–Chk1–Cdk–PP1γ axis. This pathway seems to have an important role in cell survival after DNA damage. Although the precise mechanism by which PP1γ regulates cell viability remains unknown, levels of cyclins and Cdks might be a crucial determinant of cell viability after DNA damage.

METHODS

Cell culture and adenovirus infection. HCT116 cells were cultured in McCoy's 5a medium containing 10% fetal bovine serum. HeLa cells and mouse embryonic fibroblasts were cultured in Dulbecco's modified Eagle medium containing 10% fetal bovine serum. All cells were cultured at 37 °C in 5% CO_2. Adenovirus-Cdk1AF (Niida *et al*, 2005) or LacZ (control) was used to infect HCT116 cells at multiplicity of infection 40.

Immunoblotting. Subcellular fractionation was performed as previously described (Niida *et al*, 2007). To solubilize the chromatin fraction, pellets were suspended in immunoprecipitation kinase buffer (50 mM HEPES (pH 8.0), 150 mM NaCl, 2.5 mM EGTA, 1 mM dithiothreitol, 0.1% Tween-20, 10% glycerol and protease inhibitors). For preparation of whole-cell extracts, cells were lysed in immunoprecipitation kinase buffer.

Phosphatase assay. Chromatin-bound PP1γ was solubilized and immunoprecipitated with PP1γ antibody. The precipitates were

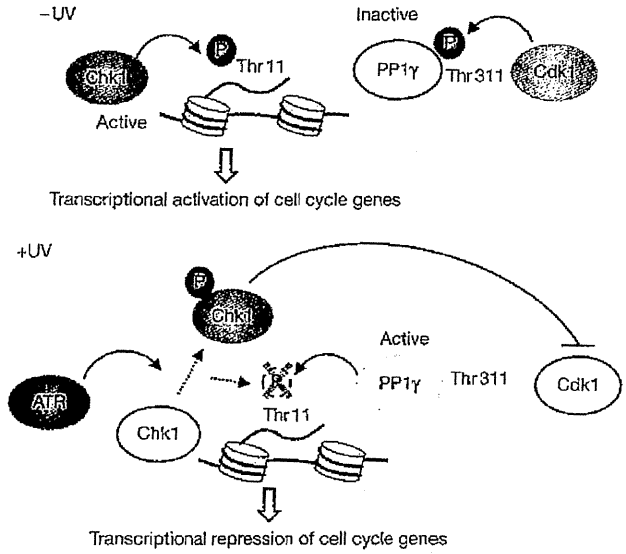

Fig 5 | Schematic model of DNA-damage-induced dephosphorylation of H3-pThr11 on the promoters of cell cycle regulatory genes. Under normal conditions (−UV), Chk1 associates with chromatin and phosphorylates H3-Thr11 to activate transcription of cell cycle regulatory genes. PP1γ is inactivated through Cdk-dependent phosphorylation at Thr311. In response to DNA damage (+UV), activated ATR phosphorylates Chk1 and the phosphorylated Chk1 then dissociates from chromatin. ATR-dependent release of Chk1 from the promoters of cell cycle regulatory genes indirectly suppresses Cdk activity, which results in activation of PP1γ through a reduction in Thr311 phosphorylation. PP1γ-mediated dephosphorylation of H3-pThr11 represses transcription of genes involved in cell cycle regulation. ATR, ataxia telangiectasia, mutated and Rad3-related; PP, protein phosphatase; UV, ultraviolet.

incubated with chromatin at 30 °C for 1 h in phosphatase buffer (10 mM HEPES, 10 mM $MgCl_2$, 1 mM $MnCl_2$ and 1 mM DTT). His-tagged wild-type PP1γ or PP1γ-Thr311A was purified from Sf9 cells and phosphatase assays were performed using a chromatin fraction as a substrate.

Knockdown experiments by siRNA transfection. HCT116 or HeLa cells were transfected with either a control siRNA (Silencer Negative Control, Ambion) or an siRNA for ATR, PP1, PP1α, PP1β, PP1γ, PP2A or Cdk1 and Cdk2 using Lipofectamine 2000 (Invitrogen). The sequences of these siRNAs were described in the supplementary Table S2 online.

Immunofluorescence. Cells were grown on glass coverslips or chamber slides, washed with phosphate buffered saline (PBS) and fixed with 2% paraformaldehyde in PBS for 15 min, and stained with the indicated antibodies diluted in 5% blocking buffer (Convance, normal serum block) and DAPI.

Quantitative real-time RT–PCR for measurement of *Cdk1*, *cyclin B1* and *cyclin A2* mRNA expressions. The RNA was extracted using ISOGEN (Wako) according to the manufacturer's protocol. Total RNAs were subjected to reverse transcription. *Cdk1*, *cyclin B1* and *cyclin A2* mRNA levels were measured by Taqman quantitative PCR, normalized to *GAPDH* gene expression and expressed relative to the un-irradiated sample.

MTT assay. HCT116 cells were incubated with medium containing MTT solution (0.5 mg/ml) for 4 h. After removing the medium, cells were incubated with DMSO and the optical density of the resultant supernatant was measured at 535 nm.

Antibodies. The antibodies used for immunoblotting were ATR (sc-1887; Santa Cruz Biotechnology), β-actin (ab6276; Abcam), Chk1 (sc-8408 and sc-56291; Santa Cruz Biotechnology), Myc (sc-789 and sc-40; Santa Cruz Biotechnology), Cdk1 (sc-54; Santa Cruz Biotechnology), Cdk2 (sc-163; Santa Cruz Biotechnology), FLAG (M2; Sigma), H3 (ab1791; Abcam), IKKα (sc-7182; Santa Cruz Biotechnology), H3 (9715; Cell Signaling Technology), pT11 (ab5168; Abcam), PP1 (sc-7482; Santa Cruz Biotechnology), pThr320-PP1 (2581; Cell Signaling Technology), PP2A (05-421; Upstate), PP1α (06-221; Upstate), PP1β (ab53315; Abcam) and PP1γ (sc-6108; Santa Cruz Biotechnology, 07-1298; Millipore).

Supplementary information is available at EMBO *reports* online (http://www.emboreports.org).

ACKNOWLEDGEMENTS

We thank P.M. Carr, D. Zineldeen and M. Delhase for critical reading of this paper; and Y. Chiba, S. Tsubaki, Y. Kawada, T. Misaki, Y. Koshiyama and C. Yamada-Namikawa for technical assistance. This study was supported in part by a Grant-in-Aid for Scientific Research (B) and the project for realization of regenerative medicine, by the Mitsubishi Foundation, by the Naito Memorial Foundation and by the Toyoaki Foundation (to M.N.), by the Mochida Memorial Foundation, Shiseido Female Researcher Science Grant and by a Grant-in-Aid for Young Scientists (A; to M.S.).

CONFLICT OF INTEREST

The authors declare that they have no conflict of interest.

REFERENCES

Cheng A, Balczon R, Zuo Z, Koons JS, Walsh AH, Honkanen RE (1998) Fostriecin-mediated G2–M-phase growth arrest correlates with abnormal centrosome replication, the formation of aberrant mitotic spindles, and the inhibition of serine/threonine protein phosphatase activity. *Cancer Res* **58:** 3611–3619

Chowdhury D, Keogh MC, Ishii H, Peterson CL, Buratowski S, Lieberman J (2005) γ-H2AX dephosphorylation by protein phosphatase 2A facilitates DNA double-strand break repair. *Mol Cell* **20:** 801–809

Chowdhury D, Xu X, Zhong X, Ahmed F, Zhong J, Liao J, Dykxhoorn DM, Weinstock DM, Pfeifer GP, Lieberman J (2008) A PP4-phosphatase complex dephosphorylates γ-H2AX generated during DNA replication. *Mol Cell* **31:** 33–46

Dohadwala M, da Cruz e Silva EF, Hall FL, Williams RT, Carbonaro-Hall DA, Nairn AC, Greengard P, Berndt N (1994) Phosphorylation and inactivation of protein phosphatase 1 by cyclin-dependent kinases. *Proc Natl Acad Sci USA* **91:** 6408–6412

Engelberg D, Klein C, Martinetto H, Struhl K, Karin M (1994) The UV response involving the Ras signaling pathway and AP-1 transcription factors is conserved between yeast and mammals. *Cell* **77:** 381–390

Harper JW, Elledge SJ (2007) The DNA damage response: ten years after. *Mol Cell* **28:** 739–745

Hsu JY *et al* (2000) Mitotic phosphorylation of histone H3 is governed by Ipl1/aurora kinase and Glc7/PP1 phosphatase in budding yeast and nematodes. *Cell* **102:** 279–291

Keogh MC *et al* (2006) A phosphatase complex that dephosphorylates γH2AX regulates DNA damage checkpoint recovery. *Nature* **439:** 497–501

Kinoshita E, Kinoshita-Kikuta E, Koike T (2009) Separation and detection of large phosphoproteins using Phos-tag SDS–PAGE. *Nat Protoc* **4:** 1513–1521

Metzger E *et al* (2008) Phosphorylation of histone H3 at threonine 11 establishes a novel chromatin mark for transcriptional regulation. *Nat Cell Biol* **10:** 53–60

Moorhead GB, Trinkle-Mulcahy L, Ulke-Lemee A (2007) Emerging roles of nuclear protein phosphatases. *Nat Rev Mol Cell Biol* **8:** 234–244

Nakada S, Chen GI, Gingras AC, Durocher D (2008) PP4 is a γH2AX phosphatase required for recovery from the DNA damage checkpoint. *EMBO Rep* **9:** 1019–1026

Niida H, Tsuge S, Katsuno Y, Konishi A, Takeda N, Nakanishi M (2005) Depletion of Chk1 leads to premature activation of Cdc2–cyclin B and mitotic catastrophe. *J Biol Chem* **280:** 39246–39252

Niida H, Katsuno Y, Banerjee B, Hande MP, Nakanishi M (2007) Specific role of Chk1 phosphorylations in cell survival and checkpoint activation. *Mol Cell Biol* **27:** 2572–2581

Nowak SJ, Pai CY, Corces VG (2003) Protein phosphatase 2A activity affects histone H3 phosphorylation and transcription in *Drosophila melanogaster*. *Mol Cell Biol* **23:** 6129–6138

Paulson JR, Patzlaff JS, Vallis AJ (1996) Evidence that the endogenous histone H1 phosphatase in HeLa mitotic chromosomes is protein phosphatase 1, not protein phosphatase 2A. *J Cell Sci* **109:** 1437–1447

Preuss U, Landsberg G, Scheidtmann KH (2003) Novel mitosis-specific phosphorylation of histone H3 at Thr11 mediated by Dlk/ZIP kinase. *Nucleic Acids Res* **31:** 878–885

Sancar A, Lindsey-Boltz LA, Unsal-Kacmaz K, Linn S (2004) Molecular mechanisms of mammalian DNA repair and the DNA damage checkpoints. *Annu Rev Biochem* **73:** 39–85

Shi Y, Manley JL (2007) A complex signaling pathway regulates SRp38 phosphorylation and pre-mRNA splicing in response to heat shock. *Mol Cell* **28:** 79–90

Shimada M, Nakanishi M (2008) Checkpoints meet the transcription at a novel histone milestone (H3-T11). *Cell Cycle* **7:** 1555–1559

Shimada M, Niida H, Zineldeen DH, Tagami H, Tanaka M, Saito H, Nakanishi M (2008) Chk1 is a histone H3 threonine 11 kinase that regulates DNA damage-induced transcriptional repression. *Cell* **132:** 221–232

Smits VA, Reaper PM, Jackson SP (2006) Rapid PIKK-dependent release of Chk1 from chromatin promotes the DNA-damage checkpoint response. *Curr Biol* **16:** 150–159

Swingle M, Ni L, Honkanen RE (2007) Small-molecule inhibitors of Ser/Thr protein phosphatases: specificity, use and common forms of abuse. *Methods Mol Biol* **365:** 23–38

Trinkle-Mulcahy L, Andersen J, Lam YW, Moorhead G, Mann M, Lamond AI (2006) Repo-Man recruits PP1γ to chromatin and is essential for cell viability. *J Cell Biol* **172:** 679–692

Vassilev LT, Tovar C, Chen S, Knezevic D, Zhao X, Sun H, Heimbrook DC, Chen L (2006) Selective small-molecule inhibitor reveals critical mitotic functions of human CDK1. *Proc Natl Acad Sci USA* **103:** 10660–10665

Walsh AH, Cheng A, Honkanen RE (1997) Fostriecin, an antitumor antibiotic with inhibitory activity against serine/threonine protein phosphatases types 1 (PP1) and 2A (PP2A), is highly selective for PP2A. *FEBS Lett* **416:** 230–234

Zhan Q, Carrier F, Fornace Jr AJ (1993) Induction of cellular p53 activity by DNA-damaging agents and growth arrest. *Mol Cell Biol* **13:** 4242–4250

Cancer Science
The official journal of the Japanese Cancer Association JCA

Review Article

Mechanisms of dNTP supply that play an essential role in maintaining genome integrity in eukaryotic cells

Hiroyuki Niida, Midori Shimada, Hiroshi Murakami and Makoto Nakanishi[1]

Department of Cell Biology, Graduate School of Medical Sciences, Nagoya City University, Mizuho-ku, Nagoya, Japan

(Received June 21, 2010/Revised August 10, 2010/Accepted August 14, 2010/Accepted manuscript online August 18, 2010/Article first published online September 28, 2010)

Optimization of intracellular concentrations of dNTPs is critical for the fidelity of DNA synthesis during DNA replication and repair because levels that are too high or too low can easily lead to increased rates of mutagenesis. Recent advances in the analysis of intracellular concentrations of dNTPs have suggested that eukaryotes use diverse mechanisms in supplying dNTPs for DNA synthesis during DNA replication and repair. The enzyme ribonucleotide reductase (RNR) is a key enzyme involved in the synthesis of dNTPs. We found that Tip60-dependent recruitment of RNR at sites of DNA damage is essential for supplying a sufficient amount of dNTPs for mammalian DNA repair. In this review, we focus on recent findings related to RNR regulation in eukaryotes of the dNTPs supplied for DNA synthesis. We also discuss the effect of this regulation on mutagenesis and tumorigenesis. (*Cancer Sci* 2010; 101: 2505–2509)

Ribonucleotide reductase (RNR) catalyzes the substitution of the 2′hydroxyl group of a ribonucleoside diphosphate with hydrogen, resulting in a deoxyribonucleoside diphosphate (dNDP) (Fig. 1A).[1] The minimal form of this enzyme is an a2b2 heterotetramer, but its higher order forms (a6b6 or a6b2) also exist as active enzymes.[2,3] In mammalian cells, the a-protein and b-protein are referred to as the R1 protein and R2 protein, respectively. The R1 protein (90 kDa) carries the active site as well as binding sites for allosteric effectors. The smaller R2 protein (45 kDa) contains an Fe–O–Fe center, which generates a tyrosyl-free radical. During catalysis, this radical is continuously shuttled to a cysteine residue in the active site.[4] Mammalian cells possess a single large subunit, *R1* and two distinct small subunits, *R2* and *p53R2*, the latter being induced by DNA damage in a manner dependent on p53 (Fig. 1A).[5] Similarly, the RNR of budding yeast contains two large subunits of *Rnr1* and one each of the small subunits *Rnr2* and *Rnr4*.[6] The expression of *Rnr3*, another large subunit, is highly elevated after DNA damage, suggesting its role in DNA repair,[7] although the level of Rnr3 protein even after DNA damage never reaches more than one-tenth of the Rnr1 protein level and a complex between Rnr3 and the Rnr2/Rnr4 heterodimer has a very low catalytic activity.[8] Intriguingly, the Rnr3-catalyzed CDP reduction is significantly stimulated by dATP, indicating that Rnr3 lacks a functional allosteric activity site that allows generation of higher levels of dNTPs for DNA repair[8] (see below).

Ribonucleotide reductase is controlled by various regulatory mechanisms, such as allosteric regulation, transcriptional regulation, post-transcriptional modification, and regulation of subcellular localization.[1,4] The eukaryotic large subunit of RNR contains two allosteric sites each consisting of a polypeptide capable of binding to effectors (dNTP or NTP). One of these is the specificity site that monitors balance among the four dNTPs and adjusts its activity to maintain their ratio, and the other is the activity site that regulates the total dNTP pool size by monitoring the dATP/ATP ratio. Both sites are required for maintaining all dNTPs at the correct overall levels (Fig. 1B).[9] In the case of DNA damage, in order to produce higher levels of dNTPs, it might be possible that either the ATP level may also increase or negative feedback regulations may be suppressed through unknown mechanisms. A failure of dATP feedback inhibition in budding yeast Rnr1 mutants results in a drastic increase in the dNTP pool during DNA damage.[10]

In addition to RNR, thymidylate synthase (TS) is a key enzyme in the synthesis of 2′-deoxythymidine-5′-monophosphate (dTMP) by catalyzing the methylation of 2′-deoxyuridine-5′-monophosphate (dUMP). Thymidylate synthase provides the sole intracellular *de novo* source of dTMP. The hydrolysis of dUTP to dUMP is catalyzed by dUTPase and the resultant pyrophosphate simultaneously provides substrate to TS. In addition, 2′-deoxycytidine-5′-monophosphate (dCMP) deaminase may produce dUMP by the deamination of dCMP. Nucleotide diphosphate kinases (NDPK) are also required for dNTP synthesis through phosphorylation of dNDPs. Therefore, these enzymes should also play an important role in the balanced supply of dNTPs for DNA synthesis. In this review, we summarize recent findings on the regulation of the dNTPs supplied for DNA synthesis. An insufficient or unbalanced supply of dNTPs into DNA strands can result in genetic abnormalities and cell death.[11] Implications of dNTP supply related to carcinogenesis are also discussed.

Mechanism of dNTP supply during DNA replication and repair in yeasts

In budding yeast, dNTP levels during DNA replication are approximately threefold higher than in G_1 phase.[10] Ribonucleotide reduction in budding yeast shows maximum activity in S phase, which is explained by the cell cycle-dependent expression of the *Rnr1* gene.[12] There is more than a 10-fold fluctuation in *Rnr1* mRNA concentrations in coordination with the induction of the *POL1* gene during the cell cycle, whereas the *Rnr2* transcript shows only a twofold fluctuation. Similarly, *cdc22*^{R1} and *suc22*^{R2} are also induced transcriptionally at the G_1/S transition by the transcription factor MBF in fission yeast.[13] Importantly, a constitutively high dNTP concentration due to a mutation in the allosteric activity site of Rnr1 arrests the cell cycle at late G_1 phase and has an effect on origin

[1]To whom correspondence should be addressed.
E-mail: mkt-naka@med.nagoya-cu.ac.jp

doi: 10.1111/j.1349-7006.2010.01719.x

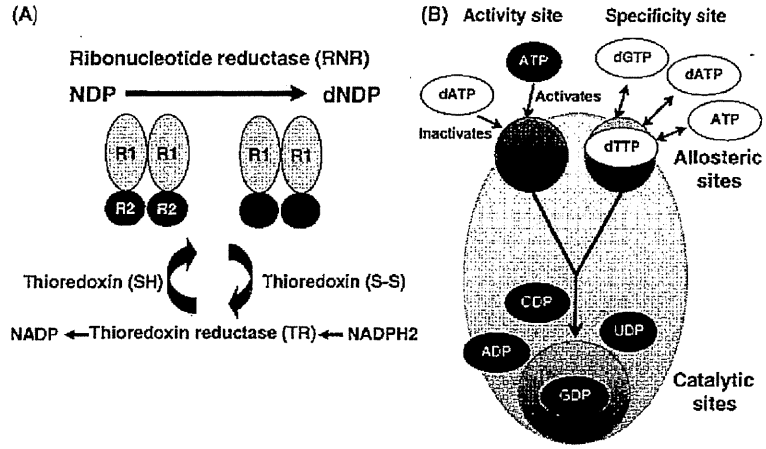

Fig. 1. Ribonucleotide reductase (RNR) and its allosteric regulation. (A) The enzyme RNR catalyzes the *de novo* synthesis of dNTPs. Catalysis of ribonucleoside 5′-diphosphate (NDP) involves a reduction at the 2′-carbon of ribose 5-phosphate to form the 2′-deoxy derivative-reduced 2′-deoxyribonucleoside 5′-diphosphate (dNDP). This reduction is initiated with the generation of a free radical. Following a single reduction, RNR requires electrons donated from the dithiol groups of the protein thioredoxin. Regeneration of thioredoxin occurs when nicotinamide adenine dinucleotide phosphate (NADPH) provides two hydrogen atoms that are used to reduce the disulfide groups of the thioredoxin protein. (B) Allosteric regulation of RNR. RNR is activated by binding ATP or inactivated by binding dATP to the activity site located on the large subunit Rnr1 (R1). When the enzyme is activated, substrates are reduced if the corresponding effectors bind to the allosteric substrate specificity site as follows. When dATP or ATP is bound at the allosteric site, the enzyme accepts UDP and CDP into the catalytic site. When dGTP is bound, ADP enters the catalytic site. When dTTP is bound, GDP enters the catalytic site. The substrates (UDP, CDP, ADP, and GDP) are converted to dNTPs. R2, small subunit Rnr2-Rnr4.

firings,[14] suggesting that fluctuation in the dNTP concentration controls the initiation of DNA replication.

The dNTP levels during the DNA damage response are approximately four-fold higher than the levels at S phase.[10] In response to DNA replication stress or DNA damage, the transcription of RNR genes increases rapidly through activation of the DNA damage response pathway, which includes the Mec1-Rad53-Dun1 kinase cascade, and the Rad3-Cds1 and/or Rad3-Chk1 pathways in budding and fission yeasts, respectively.[15,16] Upon DNA damage, Mec1 and Rad53 activate Dun1, which in turn leads to hyperphosphorylation of the Crt1 repressor.[17] This repressor encodes a DNA-binding protein that recruits and forms a complex with the general repressors Ssn6 and Tup1 to the promoters of *RNR* genes. Hyperphosphorylation of Crt1 prevents its DNA binding, providing the mechanism for transcriptional induction of *RNR* genes in response to DNA damage or DNA replication stress.[17] The *FSH3* gene is also a target of Crt1.[18] Although the exact function of family of serine hydrolases (FSH) remains unknown, it shares significant homology with dihydrofolate reductase, suggesting the interesting scenario that the activation of the Mec1-Rad53-Dun1-Crt1 pathway upon DNA damage results in derepression of the *FSH3* gene. The induced FSH activity then leads to increased tetrahydrofolate and N^{10}-methylene tetrahydrofolate pools that enhance dNTP synthesis. In addition to Crt1, Nrm1, a corepressor of MBF, is also involved in transcriptional induction of $cdc22^{R1}$ after DNA replication stalling in fission yeast.[19] In response to DNA replication block, Cds1, activated by Rad3, phosphorylates Nrm1 leading to its dissociation from MBF, which in turn results in induction of MBF-dependent transcripts, such as $cdc22^{R1}$.

Dun1 also upregulates RNR activity through regulating Sml1. Sml1 is an inhibitor of the RNR complex which binds to the large subunit of RNR through its C-terminal portion.[20] Sml1 is phosphorylated by Dun1 and degraded after DNA damage in a Mec1-Rad53-Dun1-dependent manner.[21] The degradation of Sml1 causes it to lose its ability for RNR inhibition. This strongly suggests that Dun1 kinase functions as the last step in the Mec1/Rad53 cascade to remove Sml1 during S phase and after DNA damage.

Another level of RNR regulation has been reported in which subcellular localization of RNR subunits plays a pivotal role in the formation of an active RNR complex in budding yeast.[22,23] The small subunit Rnr2-Rnr4 localizes in the nucleus, whereas the large subunit Rnr1 is cytoplasmic throughout the cell cycle. After DNA damage or during S phase, the Rnr2-Rnr4 subunit enters into the cytoplasm enabling its binding to Rnr1, to form an active complex. Under unperturbed conditions or outside of S phase, Dif1 directly binds to the Rnr2-Rnr4 complex through a Hug domain,[24,25] which is a conserved domain present among Rnr-inhibitor homologs, such as Spd1,[26] Sml1,[27] and Hug1. Dif1 binding to Rnr2-Rnr4 promotes its nuclear import. Imported Rnr2-Rnr4 then forms a complex with Wtm1, which anchors the complex in the nucleus (Fig. 2).[28,29] In the presence of DNA damage, the association of Rnr2-Rnr4 with Wtm1 is disrupted. The Dif1 protein level is significantly lowered during S phase[24] and in response to DNA damage, as Dun1 directly phosphorylates Dif1, which leads to Dif1 inactivates and triggers its degradation. The reduction in Dif1 after DNA damage or during S phase allows Rnr2-Rnr4 to move into the cytoplasm.

Very recently, Nestoras *et al.*[30] reported that although, in fission yeast, Spd1 functions to promote nuclear import of $Suc22^{R2}$ as Dif1 does in budding yeast, it also regulates RNR activity at multiple levels, such as direct inhibition of RNR activity and modulation of RNR complex architecture. Intriguingly, using several lines of mutant Spd1, they clearly demonstrated that the major function of Spd1 in regulating dNTP synthesis is unrelated to its role in nuclear sequestration of $Suc22^{R2}$. Therefore, the molecular system in which subcellular localization of RNR subunits enables the generation of an active RNR complex, and thereby regulates dNTP synthesis, may be specifically used in budding yeast.

Mechanisms of dNTP supply during DNA replication and repair in mammals

During DNA replication, in mammalian cells the whole dNTP pool is increased to a level 20-fold higher than the level in G_1

doi: 10.1111/j.1349-7006.2010.01719.x

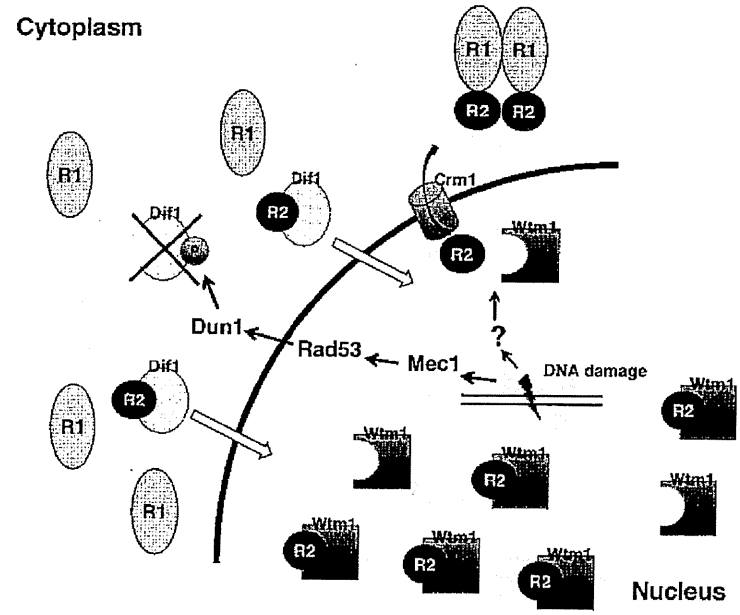

Fig. 2. Regulation of subcellular localization of ribonucleotide reductase (RNR) in budding yeast. The small subunit Rnr2-Rnr4 (R2) localizes at the nucleus, whereas the large subunit Rnr1 (R1) is cytoplasmic outside of S phase. After DNA damage or during S phase, the Rnr2-Rnr4 subunit enters the cytoplasm enabling it to bind to Rnr1, forming an active complex. Dif1 directly binds to the R2 complex which promotes the import of R2 into the nucleus. The imported R2 then forms a complex with Wtm1, which anchors the complex in the nucleus. In the presence of DNA damage, the association of R2 with Wtm1 is disrupted. Furthermore, DNA damage-induced activation of the Mec1-Rad53-Dun1 axis directly phosphorylates (P) Dif1, which inactivates and triggers its degradation. A reduction in Dif1, together with the dissociation of R2 from Wtm1 after DNA damage, allows R2 to enter the cytoplasm.

phase cells.[31] This increase is mainly regulated at transcriptional and post-transcriptional levels. The transcription of *R1* and *R2* genes is cell cycle-regulated, with undetectable mRNA levels in G_0/G_1 phase and maximal levels in S phase when cells are arrested at a quiescent state by serum starvation and then released into G_1 phase by serum addition.[32] Promoter–reporter analysis revealed that the mouse *R1* gene promoter is TATA-less and its S phase-specific activation is partly regulated by YY1.[33] The mouse *R2* gene promoter possesses a typical TATA box and its S phase-specific activation is regulated by transcriptional activation through the upstream activating region.[34] Another *R2* gene, *p53R2*, was first identified as a p53-inducible gene using differential display.[5,35] Unlike *R2*, *p53R2* is constitutively expressed at a low level during the cell cycle, but is significantly induced when p53 is activated.[36] Therefore, p53R2 has been proposed to play a role in dNTP synthesis in resting cells in which R2 is undetectable. More recently, various mutations in *p53R2* have been identified in several patients with mitochondrial DNA (mtDNA) depletion syndrome.[37] Severe mtDNA depletion was also found in various tissues of *p53R2*-deficient mice that died from severe renal failure through enhancement of p53-induced apoptosis.[38] Taken together, p53R2 has a non-redundant role in supplying dNTP for mtDNA synthesis in resting cells.

R2 protein degradation at mitosis also appears to be important for S phase-specific expression of R2 protein. The mouse R2 protein specifically binds to the Cdh1-anaphase-promoting complex through its KEN box.[39] This interaction leads to polyubiquitination and degradation of R2 protein by way of proteasomes. p53R2 protein, however, lacks a KEN box.

Other enzymes involved in dNTP synthesis are also upregulated during DNA replication. Expression of NDPK and TS is induced during G_1 to S phase.[40,41] The activity of the dCMP deaminase shows periodic regulation during the cell cycle[42] and the expression of the nuclear isoform of dUTPase is induced during S phase,[43] suggesting the existence of a regulatory network of the enzymatic activities toward dTTP supplied for DNA replication.

Recent advances in the methodology of measuring dNTP have revealed that whole dNTP pools in mammalian cells are almost unchanged after DNA damage,[31] suggesting the existence of a unique mechanism in mammals by which dNTPs are compartmentalized close to the damage site during the DNA repair process, thereby providing a high local dNTP concentration (Fig. 3). Although the exact reason why mammalian cells possess this unique mechanism is not known, compartmentalization of dNTPs may be less wasteful for providing sufficient amounts of dNTPs. Alternatively, high concentrations of dNTPs outside S phase might be deleterious in mammals. We detected traces but significant signals of both R1 and R2 proteins in a chromatin fraction,[44] although both R1 and R2 predominantly localized in the cytoplasm as reported.[45] We also found that both R1 and R2 proteins accumulated very rapidly at sites of DNA damage on an evaluation using ionizing irradiation treatment and UVA microirradiation. R1 constitutively forms a complex with Tip60 histone acetyltransferase, which is rapidly recruited to DNA

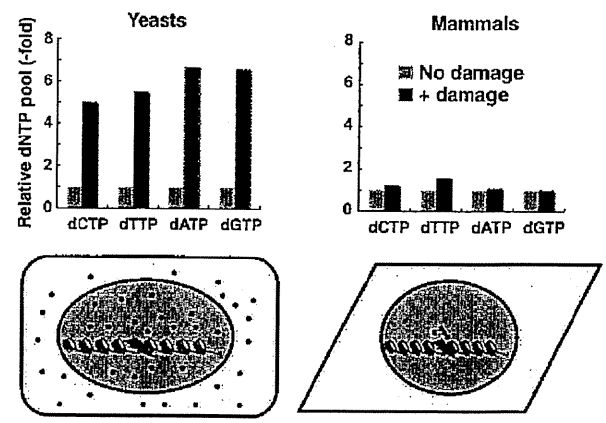

Fig. 3. Sharp contrasts between yeasts and mammals in the regulation of dNTP pools after DNA damage. After DNA damage, whole dNTP pools in mammalian cells are almost unchanged, but those in yeasts are drastically increased.[10] These observations suggest that there is a unique mechanism in mammals by which dNTPs are compartmentalized close to the damage sites during the DNA repair process, thereby providing a high local concentration. Black dots represent dNTPs (lower panels).

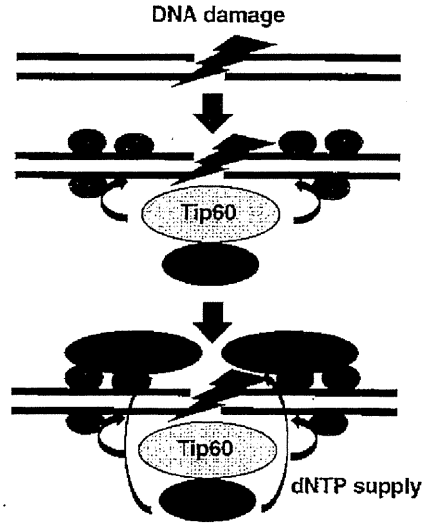

Fig. 4. Mechanism of dNTP supply to DNA damage sites in mammals After DNA damage, the Tip60/ribonucleotide reductase (RNR) complex is rapidly recruited to the damage sites. Tip60 acetylates (Ac) histone H4 surrounding these sites and this acetylation enhances recruitment of repair enzymes and several checkpoint proteins. Recruited RNR can supply sufficient amounts of dNTPs for proper DNA repair.

damage sites[46] through its chromo-domain.[47] Hence, the accumulation of R1 and R2 proteins requires an R1 interaction with Tip60 (Fig. 4). In this regard, it might be possible that Tip60 enhances the formation of active RNR complexes as Spd1 does in fission yeast.[30] Tip60-dependent recruitment of RNR to these damage sites is essential for efficient DNA repair because an active R1 mutant lacking Tip60 binding shows an impaired DNA repair. Intriguingly, recruitment of RNR is specifically required for effective DNA repair in cells with low levels of dNTPs, such as G_1 phase cells. Although Tip60-dependent recruitment of RNR is not involved in the dTTP supply to DNA damage sites, it should be noted that γ-radiation in mice significantly induced the enzymatic activity of TS as well as that of dihydrofolate reductase,[48] which may produce a sufficient amount of dTMP for DNA repair. Importantly, DNA damage has been reported to induce nuclear localization of NDPK,[49] suggesting its role in dNDPs to dNTPs conversion in DNA repair.

Implications of dNTP supply in tumorigenesis

Budding yeast RNR mutants with increased dNTP pools show increased survival following DNA damage even with higher mutation rates,[10] possibly due to reduced fidelity of the replicative polymerases and/or activation of error-prone translesion polymerases during DNA synthesis. The features of RNR underlying its essential function in dNTPs supply strongly suggest that it is involved in a tumorigenic environment and is a potential biomarker for the clinical outcome and the chemotherapeutic efficacy of anticancer drugs. Ectopic expression of R1 in ras-transformed mouse fibroblasts results in reduced anchorage-independent growth and tumor formation.[50] Increased expression of R1 in human lung cancer cells also results in reduced cellular migration, invasion, and metastasis.[51] Finally, transgenic mice overexpressing R1 show a strong suppression of carcinogen-induced lung tumor formation.[52] Thus, the high level of dNTP supply for DNA synthesis might protect mammalian cells from progressive malignant transformation.

In contrast, an insufficient level of dNTPs can lead to malignant transformation. Fission yeast mutants with reduced dNTP pools show an increased rate in spontaneous mutations, including base substitution and small insertion/deletion,[53] presumably due to recruitment of error-prone translesion polymerases to extend stalled replication forks. Tip60 is reported to be a haplo-insufficient tumor suppressor required for an oncogene-induced DNA damage response.[54] Although Tip60 is required for the tumor suppressor function of ATM, and there is still no direct evidence implicating Tip60-dependent recruitment of RNR to DNA damage sites in tumorigenesis, an insufficient dNTP supply to these sites in Tip60 heterozygote mice might explain their predisposition to cancer.

Gemcitabine (2′deoxy-2′/2′-difluorocytidine monohydrochloride), one of the principal chemotherapeutic agents in the treatment of non-small-cell lung cancer (NSCLC), is a potent and specific pyrimidine nucleoside antimetabolite with structural relatedness to deoxycytidine. Low *R1* mRNA expression was reported to be associated with a significantly longer overall survival in NSCLC patients treated with gemcitabine/cisplatin,[55–57] although the molecular basis underlying this association remains elusive. *R1* polymorphisms have also been reported to be associated with the clinical outcome in NSCLC patients treated with this drug.[58]

In summary, accumulating evidence for the physiological importance of RNR regulation in maintaining genome integrity strongly suggests that components of the pathways regulating RNR function may be potent candidates as molecular targets in novel anticancer strategies. Although the exact function of each protein in mammalian ATM-Chk2-p53-RNR signaling upon DNA damage is somewhat different from that found in yeast (Mec1-Rad53-Dun1-Crt1-RNR), conservation of these pathways is intriguing as both pathways determine sensitivity of cell survival to DNA damage agents. More importantly, *p53* and *ATM* are two of the 10 most frequently mutated genes in lung adenocarcinoma, but their mutations are mutually exclusive,[59] suggesting that mutations in *ATM* and *p53* may be independently sufficient for the loss of RNR regulation. Therefore, prospective, epidemiologic, and clinical studies are needed to delineate the effects of factors regulating RNR in carcinogenesis and during ongoing therapy in humans.

References

1 Nordlund P, Reichard P. Ribonucleotide reductases. *Annu Rev Biochem* 2006; **75**: 681–706.
2 Kashlan OB, Scott CP, Lear JD, Cooperman BS. A comprehensive model for the allosteric regulation of mammalian ribonucleotide reductase. Functional consequences of ATP- and dATP-induced oligomerization of the large subunit. *Biochemistry* 2002; **41**: 462–74.
3 Rofougaran R, Vodnala M, Hofer A. Enzymatically active mammalian ribonucleotide reductase exists primarily as an alpha6beta2 octamer. *J Biol Chem* 2006; **281**: 27705–11.
4 Kolberg M, Strand KR, Graff P, Andersson KK. Structure, function, and mechanism of ribonucleotide reductases. *Biochim Biophys Acta* 2004; **1699**: 1–34.
5 Tanaka H, Arakawa H, Yamaguchi T *et al.* A ribonucleotide reductase gene involved in a p53-dependent cell-cycle checkpoint for DNA damage. *Nature* 2000; **404**: 42–9.
6 Chabes A, Domkin V, Larsson G *et al.* Yeast ribonucleotide reductase has a heterodimeric iron-radical-containing subunit. *Proc Natl Acad Sci USA* 2000; **97**: 2474–9.
7 Elledge SJ, Davis RW. Two genes differentially regulated in the cell cycle and by DNA-damaging agents encode alternative regulatory subunits of ribonucleotide reductase. *Genes Dev* 1990; **4**: 740–51.
8 Domkin V, Thelander L, Chabes A. Yeast DNA damage-inducible Rnr3 has a very low catalytic activity strongly stimulated after the formation of a cross-talking Rnr1/Rnr3 complex. *J Biol Chem* 2002; **277**: 18574–8.

doi: 10.1111/j.1349-7006.2010.01719.x